Electronic Supporting Information for

Article

Handed mirror symmetry breaking at the photoexcited state of non-rigid anthracene-containing rotamers in achiral solvents

Puhup Puneet*[1], Sajan Singh[2], Michiya Fujiki*[3], and Bhanu Nandan*[4]

[1] Department of Textile Technology, Indian Institute of Technology Delhi, Delhi, India-110016; puhuppuneet@gmail.com

[2] Department of Textile Technology, Indian Institute of Technology Delhi, Delhi, India-110016; sajansingh1507@gmail.com.

[3] Division of Materials Science, Graduate School of Science and Technology, Nara Institute of Science and Technology (NAIST), 8916-5 Takayama, Ikoma, Nara 630-0036, Japan; fujikim@ms.naist.jp.

[4] Department of Textile Technology, Indian Institute of Technology Delhi, Delhi, India-110016; nandan@textile.iitd.ac.in.

* Correspondence puhuppuneet@gmail.com (PP), fujikim@ms.naist.jp (MF), nandan@textile.iitd.ac.in (BN)

Background and Experimental Precautions

After the first prediction of an inherent dissymmetry force existing in-universe in the mid-19th century, nowadays, this is widely known as Pasteur's great conjecture (1860, Paris). There has been a long debate among nuclear physicists, particle and sub-atomic physicists, atomic physicists, molecular scientists, and organic/inorganic/polymer/colloid chemists on whether or not it is possible to observe significant signals corresponding to molecular parity violation (MPV) owing to the extremely minimal energy difference between enantiomers, experimentally. From the viewpoint of Gibbs free energy, van't Hoff formulated that *E(left) = E(right)* in his book (1899), noting that there is no energy difference between mirror-image molecules in the ground state. It is the core concept in 20th and 21st-century chemistry.

However, after a century after the Pasteur's conjecture, the β-decay experiments of ^{60}Co→^{60}Ni nuclear reaction were designed by Wu *et al.* (*Phys. Rev*. 105, 1413-1415 (1957)) and Schopper (*Phil. Mag*., 2, 710-713 (1957) to answer the question raised by Lee and Yang (*Phys. Rev*., 104, 254-258 (1956)). The nuclear β-decay experiments proved that ^{60}Co, which is regarded as the excited state of ^{60}Ni in the ground state, spontaneously radiates left-hand γ-ray (circularly polarized light or spinning photon), left-hand (spin-polarized) electron, and right-hand (spin-polarized) anti-neutrino. Parity in the β-decay experiments, arising from weak-charge current mediated by massive W^{-} boson (80 GeV) was violated. The β-decay experiments prompted atomic physicists to think whether atomic vapors and molecular vapors reveal optical activity. In 1974, French physicists estimated theoretically the degree of circular polarization of cesium vapor, lead vapor, and molecular oxygen gas, arising from parity-violating weak neutral current (WNC) mediated by massive neutral Z^0 boson (91 GeV) (M.A. Bouchiat and C.Bouchiat, *Phys. Lett. B*, 48, 111-114 (1974)).

Actually, US physicists succeeded in measuring an optical rotation dispersion (ORD) spectrum of atomic lead vapor at 1240 nm as absorption mode (T.P. Emmons, J.M. Reeves, and E.N. Fortson, *Phys. Rev. Lett*., 51, 2089-2092 (1983)). Also, the Bouchiat team clearly detected photoluminescence-detective circular dichroism spectrum (similar to fluorescence-detective circular dichroism spectroscopy: so-called FD-CD technique that is equivalent to the present circularly polarized luminescence (CPL)) of cesium vapor by monitoring a near-infrared emission ($6P_{1/2}$–$7S_{1/2}$ transition at 1360 nm) upon circularly polarized photoexcitation of forbidden $6S_{1/2}$–$7S_{1/2}$ transition at 539 nm (M.A. Bouchiat and L. Pottier, *Science*, 234, 1203-1210 (1986)). To clearly detect parity violation at the nuclear reaction and atomic vapors, spontaneous radiation mode (β-decay and photoluminescence) from the metastable to stable states is more sensitive than absorption mode from the stable to metastable states.

The β-decay experiments further prompted several molecular physicists. In 1966, Yamagata was the first to theoretically hypothesize the degree of parity violation signals revealing extremely weak signals between mirror-image DNA and amino acid and proposed a linear amplification scheme of the weak molecular parity violation signals (Y. Yamagata, *J. Theoret. Biol*., 11, 495-498 (1966). This paper stimulated many molecular physicists and chemists, who are interested in the topic that whether molecular parity violation (MPV) hypothesis is valid and even if it is true, whether the signals and events are detectable. To our knowledge, most molecular theoretical physicists in the past and now estimated that energy difference of hypothetical mirror image rigid molecules and non-rigid molecules with rotational freedom of C–C/C–O/C-N bonds is on the order of 10^{-14} to 10^{-20} Kcal mol^{-1} in the ground state (zero-Kelvin) that is equivalent to 10^{-11}-10^{-17} *% ee*. Chemists concur that such a subtle difference is definitively out of measurable range and reproducibility when ordinary experimental setups are used. This idea appears to be consistent with *E(left) = E(right)* of mirror-image molecules in the ground state formulated by van't Hoff (1899), even if most of all MPV theory in the ground state is valid.

However, yet detailed MPV studies of non-rigid luminophoric rotamers and rigid luminophores in the photoexcited state are not reported theoretically and experimentally. Actually, mirror symmetry concept (parity conservation law) of non-rigid luminophoric rotamers in the photoexcited state is not proven yet until recently. MF, one of the authors, experimentally tested MPV hypothesis of nearly 50 non-rigid molecular luminophores in nearly 30 achiral solvents, and for comparison, four rigid achiral molecular luminophores and four rigid mirror-image molecular luminophores using well-maintained CPL and CD spectrometers (M.Fujiki, J.R.Koe, T.Mori, Y.Kimura, *Molecules,* 23, 2606 (2018), M.Fujiki, J.R.Koe, S.Amazumi, *Symmetry,* 11, 363 (2019)). Without exception, all non-rigid luminophores revealed (-)-sign CPL signals, meaning that parity violation in the photoexcited state. We observed that the (-)-sign CPL amplitude of oligo-p-phenylenes ($N = 2\text{-}6$) and oligofluorenes ($N = 2\text{-}7$) almost linearly increased with the number of N, as predicted by Yamagata. For comparison, we confirmed that the rigid achiral and rigid mirror-image luminophores revealed no detectable CPL signals and mirror-image CPL signals, respectively. This means that the *E(left) = E(right)* in the ground state is still applicable to mirror-image molecules in the photoexcited state. MF gave a possible explanation that mirror-symmetric double-well potential in the photoexcited state turns to dissymmetric one due to a handed tunneling mechanism mediated by weak neutral current mediated by Z^0 boson, while mirror-symmetric double-well potential in the ground state is keeping mirror-symmetric one. Although electronic energy potential in the ground state is even-function, while electronic potential in the photoexcited state is odd-function.

Recently, Vauthey *et al*., found the excited-state symmetry breaking of donor-acceptor-donor (D-A-D) type, the two-fold symmetrical quadrupolar molecule at the S1 state using ultrafast transient IR spectroscopy (*J. Am. Chem. Soc*., 138, 4643-4679 (2016). The excited-state symmetry breaking of D-A-D and A-D-A type rotamers is currently a hot topic in photophysics and photodynamics of several luminophoric rotamers (Vauthey *et al*., *J. Phys. Chem. Lett*., 8, 5878 (2017); Vauthey *et al*., *J. Phys. Chem. Lett*., 10, 2944-2948 (2019); Kobayashi, Mitsui, and coworkers, *J. Phys. Chem. C*, 37, 21295-21307 (2018)). Although their findings are based on careful analysis of solvent-polarity dependent photodynamics (Lippert-Mataga analysis) and viscosity dependency of the surrounding media, this topic does not mention about a handed mirror symmetry breaking at the lowest excited-state (does not mean parity violation at S_1 state). Studies of our photoexcited-state mirror symmetry breaking and their excited-state symmetry breaking commonly arose from re-organization process in the photoexcited non-rigid molecules in a fluidic medium, in line with Kasha's rule.

Herein, our experiment reports comprehensively, for the first time, the parity violation at S_1 state of three new non-rigid luminophores, anthracene-core rotamers when dissolved in several achiral solvents by means of CPL spectroscopy to detect a subtle imbalance in population between left- and right-hand molecules in the S_1 state. It is emphasized that, *without exception, dominant-negative sign CPL signals are found to complement relative quantum efficiency, fluorescence lifetime, radiative decay rate, and transition dipole moment of anthracene-core and bi-anthracene core rotamers as a function of solvent viscosity, while we confirmed that rigid achiral luminophores and rigid chiral luminophores had no detectable CPL and mirror-image CPL signals, respectively*. Our study should provide substantial experimental evidence to the molecular parity violation (MPV) hypothesis. With this study, we advocate that a possible origin for the handed chiral bias in life on Earth would be "a handed weak-nuclear-force origin necessity scenario" but not "several by-chance mechanisms."

Also, systematic experiments were performed to avoid any artifacts and reliable performance of the CPL and CD instruments. In order to measure CPL and CD spectra of any sample, we confirmed in advance that our CPL instrument (JASCO CPL-200) and CD instrument (JASCO J820) used in this work are routinely maintained by highly trained JASCO engineers, and guaranteed the precise measurements. Further, the CD and CPL measurements were performed for naphthalene (1), anthracene (2), tetracene (3), pyrene (4), D_{2h}-symmetrically fused aromatic molecules, and no-CD and no-CPL signals were confirmed in achiral solutions (M. Fujiki *et al*. *Molecules*, 23, 2306 (2018)). Moreover, mirror-image spectra (the same absolute magnitude, the same wavelengths (CD, UV-vis) and (CPL, PL) for *D*-/*L*-camphor and twisted binaphthyl (M. Fujiki *et al*. *Molecules*, 23, 2306 (2018)), were observed. These results verify the authenticity of the CD and CPL measurements which produced mirror image (negative and positive sign CPL) for *D*-/*L*-camphor and twisted binaphthyl owing to the high barrier of $\Delta E_{\pm}$, whereas, no CD and no CPL signals were observed for rigid molecules.

Moreover, the effect of the external magnetic field at CD and CPL instruments is ca. 0.3 Gauss (3×10^{-4} Tesla) by measuring a Hand-held Gaussmeter (Lakeshore Cryonics, model 410. Japanese vendor, Toyo Technica (Tokyo, Japan). The small magnetic field does not affect CD and CPL measurements significantly. The earth-origin magnetic field inside of the measurement chamber made of non-magnetic metals is expected to be less than 0.1 Gauss. To see the magnetic field of CD and CPL (MCD and MCPL), at least 3000 Gauss (0.3 Tesla) is needed.

However, we did not perform any measurements to overrule the possibility of interaction of cosmic rays, but our CD and CPL instruments are inside room, and it is shielded by concrete walls and floor, located on the 3rd floor of the six-floor building (NAIST, JAPAN). The effect of a cosmic ray would be extremely minimal, except neutrino and anti-neutrino coming from the cosmic origin, solar origin, earth-crust origin (^{40}K, ^{232}Th, ^{238}U), and nuclear power station origin (^{238}U). Although there are two nuclear power stations at Takahama and Ooi, Kansai electronic Power Co, Japan, they are about 200 Km away from Nara (experimental location). Since cross-section between handed spinning neutrino/antineutrino and matters are extremely small, the neutrino origin CPL signal from DSA, DSBA, and DSBP is undetectable. Practically, it is close to impossible to have an effect of the nuclear power station origin anti-neutrino at Nara which is extremely negligible. Scientists are working to achieve the deliberate interaction of neutrino and anti-neutrino by designing big-observatory setups owing to the difficulties associated with it. Therefore the probability of interaction of cosmic rays is extremely low and should not have any effect on CPL measurements.

The explained experimental results and precautions which were taken, should rule out the possibility of experimental errors, although, to cross-check the reproducibility of our results obtained, we requested JASCO corporation to measure the CPL spectra of Exalite-428 (commercial rotamer used for dye laser) which is a π–conjugated rotamer and for twisted binaphthyl ((*S*)- and (*R*)-1,1′-binaphthyl-2,2-hydrogen phosphate (TCI) (*R*/*S*-11). We observed that these experimental results independently produced by JASCO were in complete agreement of our results obtained in our lab (M. Fujiki *et al*. *Molecules,* 23, 2306 (2018)).

Chiroptical Analysis

The dissymmetry factor of the circular polarization at the S0 state (gabs) was evaluated as gabs = (εL – εR) / [1/2(εL + εR)], where εL and εR are the extinction coefficients for l- and r-CP light, respectively. The dissymmetry factor of the circular polarization at the S1 state (glum) was evaluated as glum = (IL –IR) / [1/2(IL + IR)], where IL and IR are the signals for l- and r-CP light under the unpolarized incident light, respectively. The parameter gabs was experimentally determined using the expression $\Delta\varepsilon/\varepsilon$ = [ellipticity (in mdeg)/32,980]/[absorbance] at the CD extremum, similar to the parameter glum, calculated as $\Delta I/I$ = [ellipticity (in mdeg)/(32,980/ln10)]/[total PL intensity (in Volts)] at the CPL extremum.

Reagents and achiral Solvents used

9,10-Dibromobianthracene (Sigma Aldrich, 98%), 10,10'-Dibromo-9,9'-bianthracene (Sigma Aldrich, 98%), 4,4'-Dibromo-1,1'-biphenyl (Sigma Aldrich, 98%), K3PO4 (Sigma Aldrich, >98%), Pd(OAc)2, N,N-dimethylacetamide (Sigma Aldrich, anhydrous, 99.8%).

The solvent viscosity in cP (temperature in °C) with the vendors were identical to those in refs. 42 and 43 of the manuscript.

Methanol (FUJIFILM Wako (Osaka, Japan), 0.55), ethanol (FUJIFILM Wako, 1.09), n-propanol (Sigma-Aldrich, 1.96), n-butanol (FUJIFILM Wako, 2.59), n-pentanol (Sigma-Aldrich, 3.47), n-hexanol (Sigma-Aldrich, 4.59), n-heptanol (FUJIFILM Wako, 5.97), n-octanol (FUJIFILM Wako, 7.59), n-nonanol (Sigma-Aldrich, 9.51), n-decanol (Sigma-Aldrich, 11.50), ethylene glycol (FUJIFILM Wako, 16.1, n-undecanol (Sigma-Aldrich, 16.95), 1,3-propandiol (FUJIFILM Wako, 33.0), 1,4-butanediol (FUJIFILM Wako, 71.0), chloroform (Dotite, 0.55), and D2O (FUJIFILM Wako, 0.96).

1. NMR and Mass spectra of synthesized umoniphores:

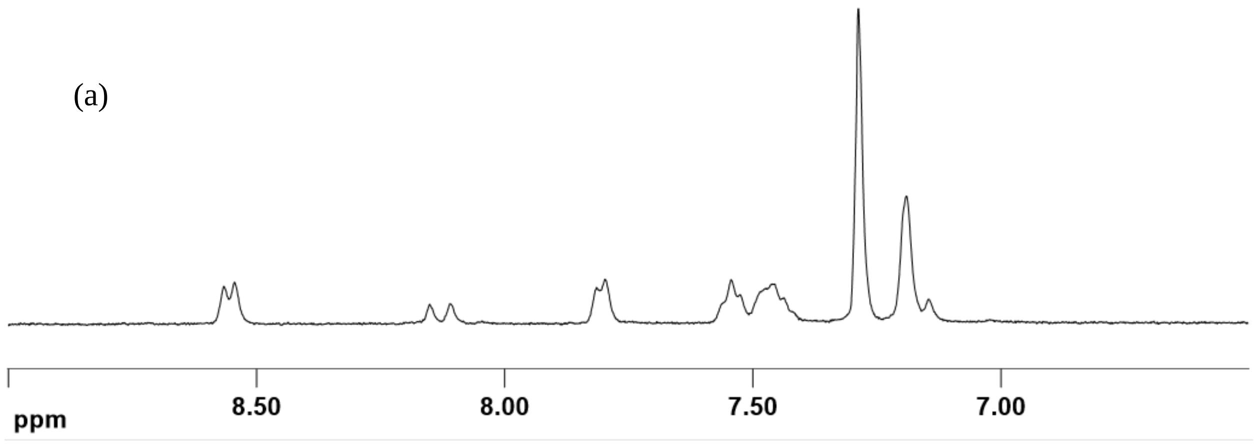

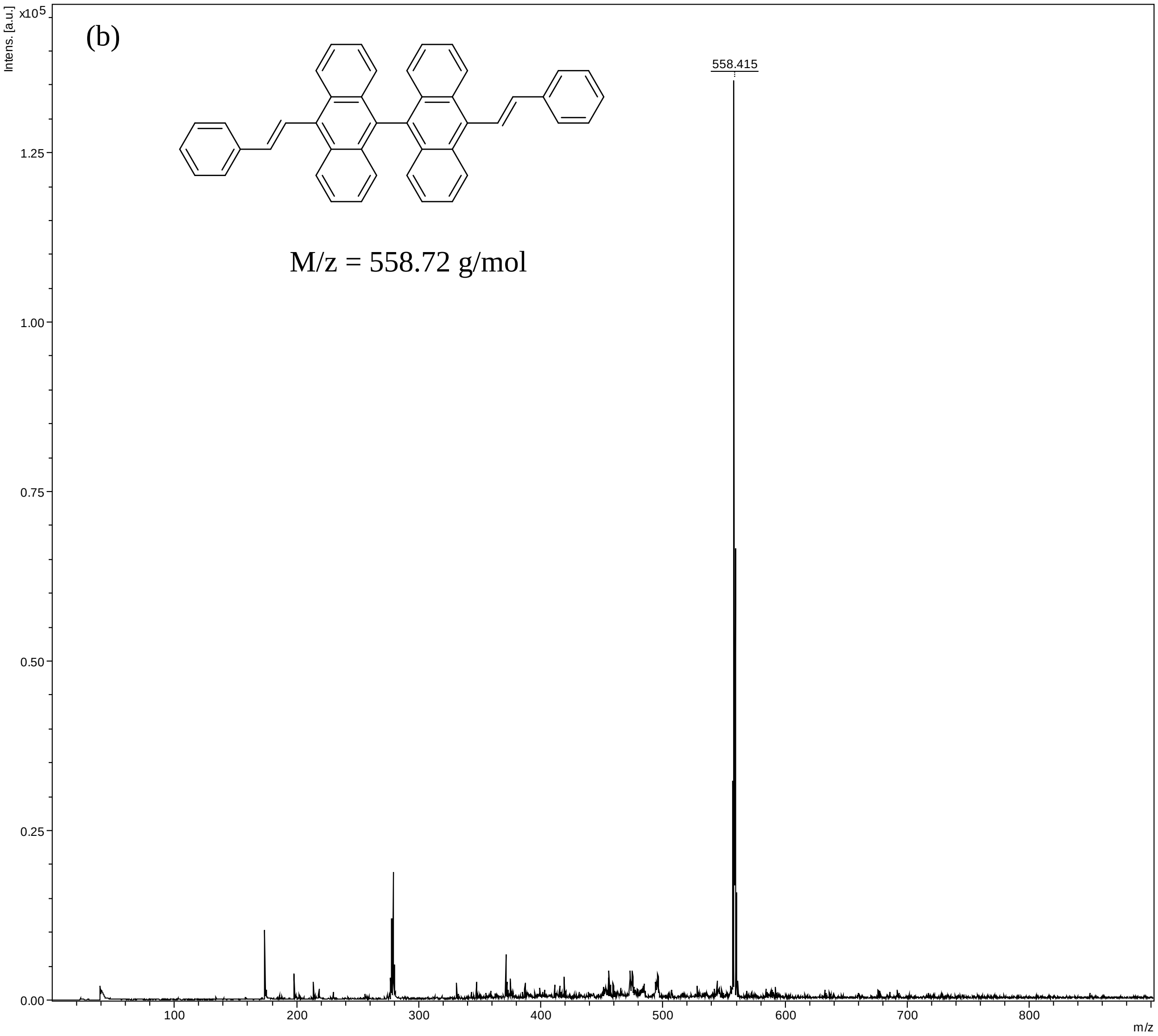

Fig, S1: ^{1}H-NMR spectrum (a) and MALDI-TOF spectrum (b) of DSBA.

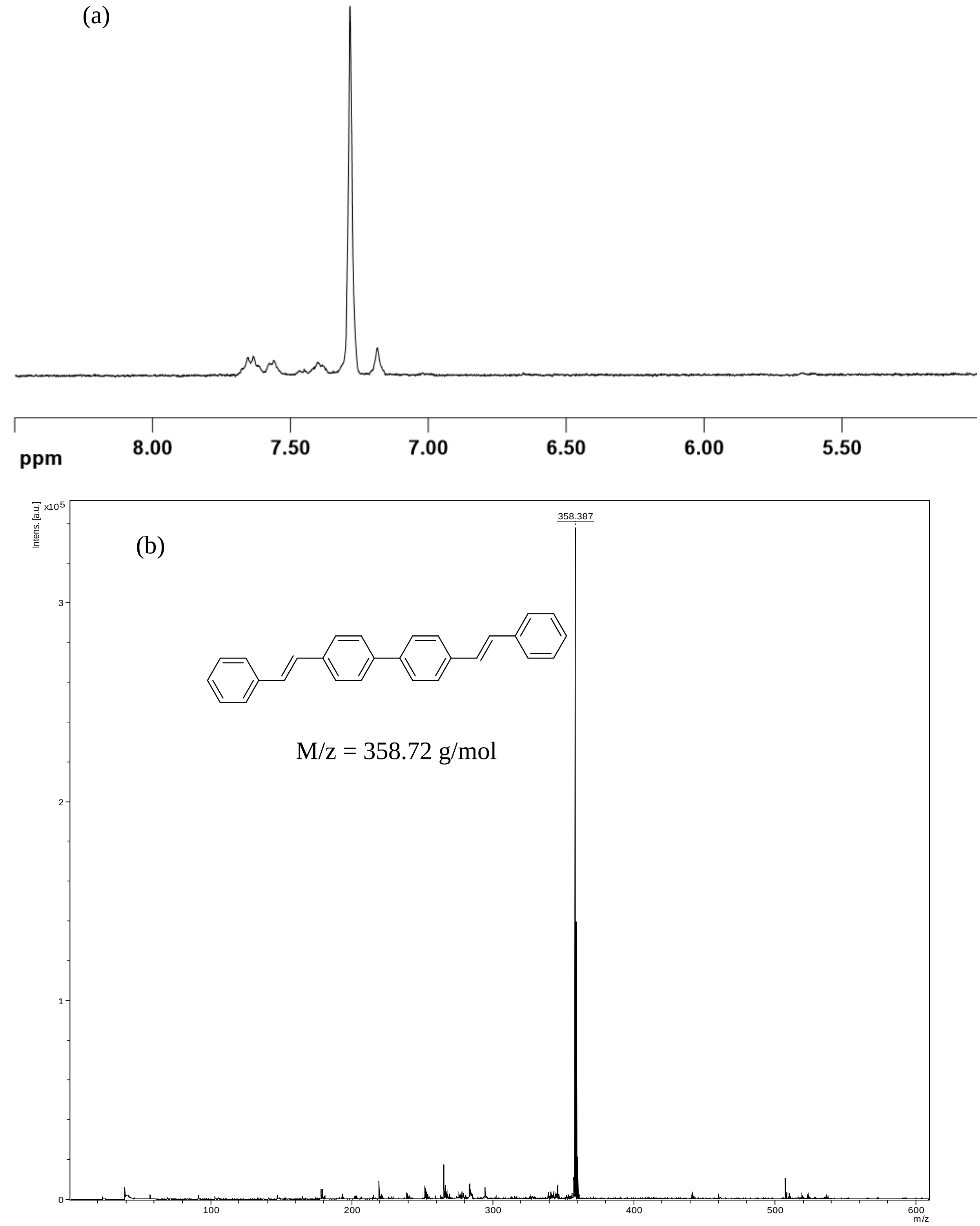

Fig, S2: ^{1}H-NMR spectrum (a) and MALDI-TOF spectrum (b) of **DSBP**.

2. CPL and CD spectra of various samples in solutions:

(*a*)

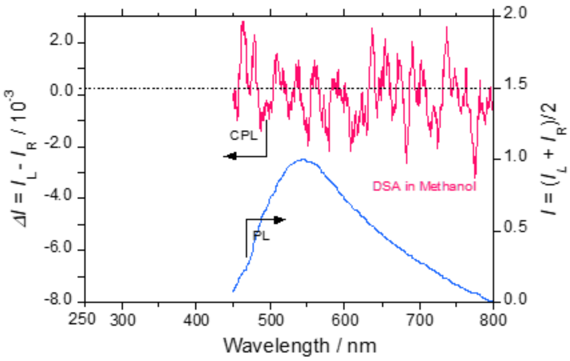

(*b*)

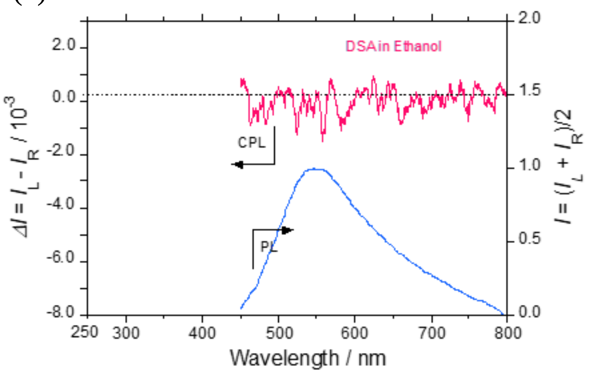

(*c*)

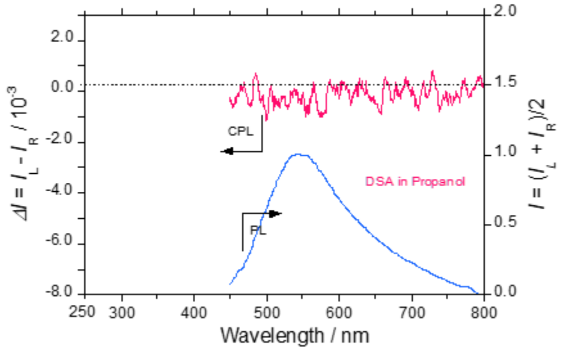

(*d*)

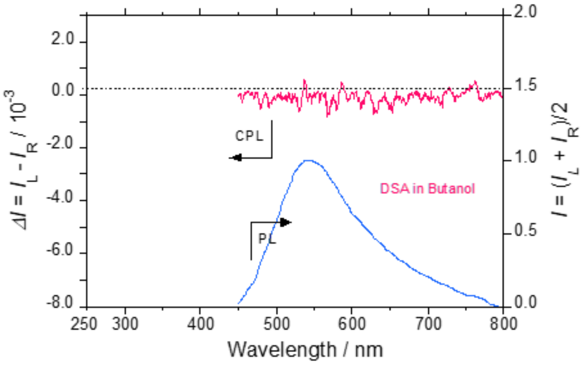

(*e*)

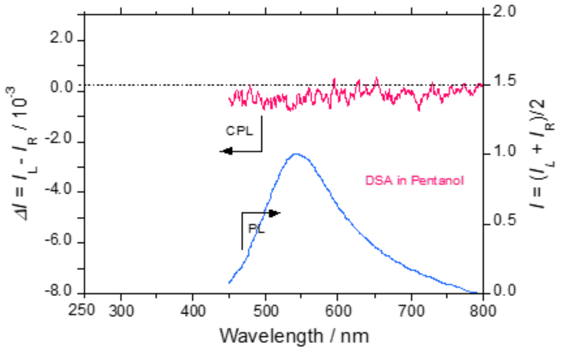

(*f*)

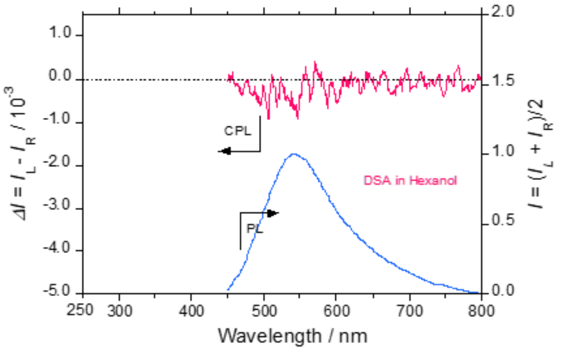

(*g*)

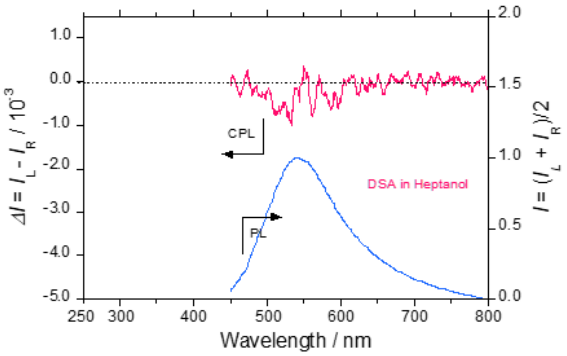

(*h*)

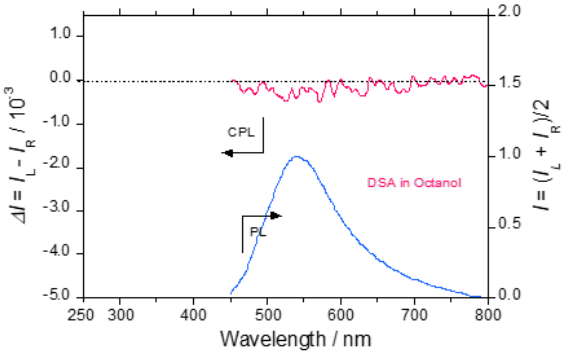

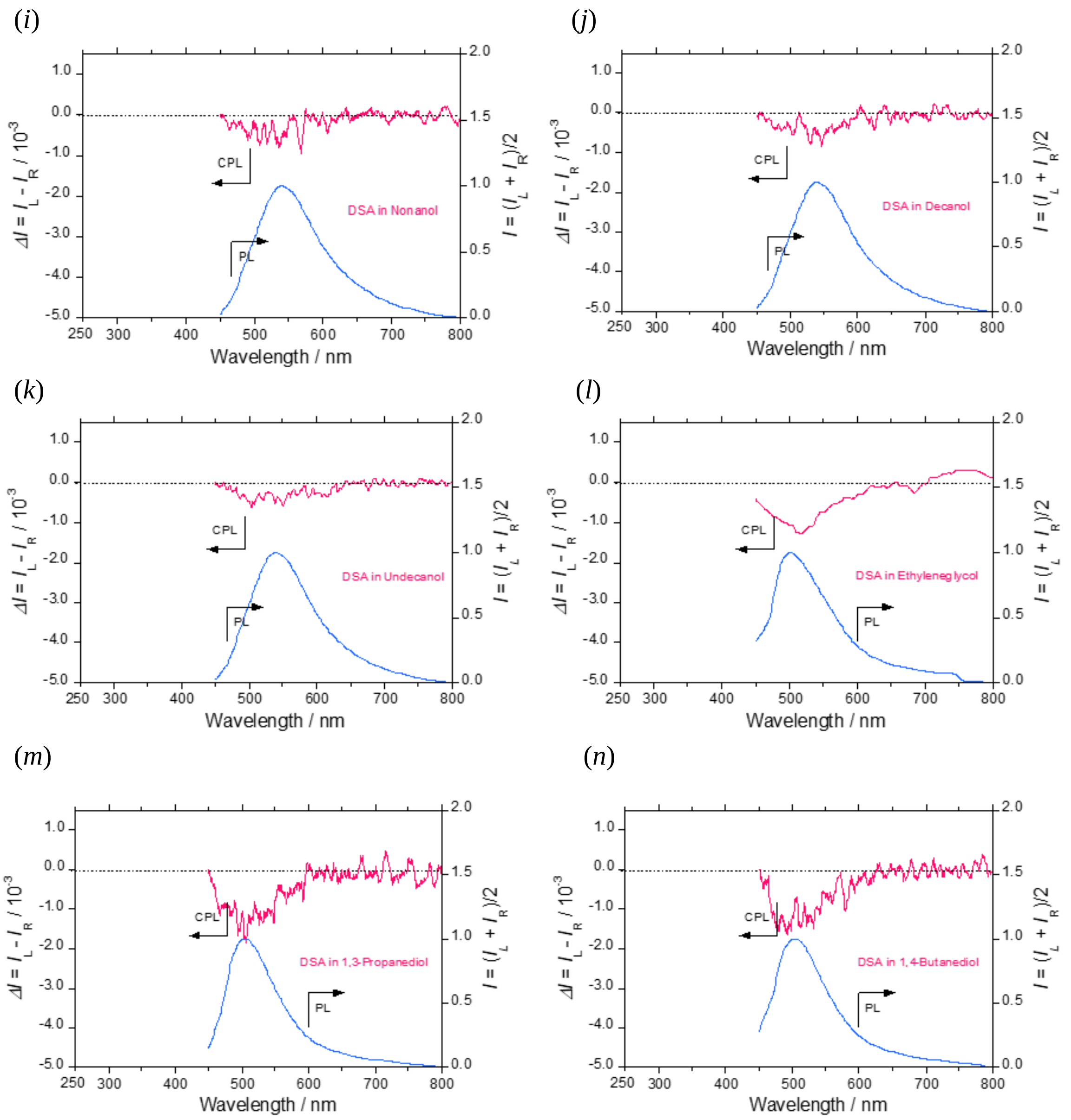

Fig. S3: CPL spectra of **DSA** in Methanol (a), Ethanol (b), *n*-Propanol (c), *n*-Butanol (d), *n*-Pentanol (e), *n*-Hexanol (f), *n*-Heptanol (g), *n*-Octanol (h), *n*-Nonanol (i), *n*-Decanol (j), *n*- Undecanol (k), Ethyleneglycol (l), 1,3-Propanediol (m), 1,4-Butanediol (n).

(*a*)

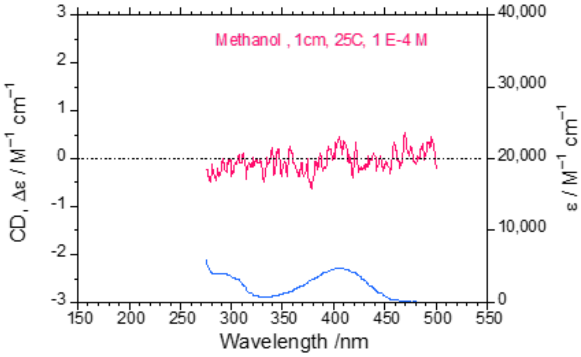
Methanol , 1cm, 25C, 1 E-4 M
CD, Δε / M⁻¹ cm⁻¹
3
2
1
0
-1
-2
-3
ε / M⁻¹ cm⁻¹
40,000
30,000
20,000
10,000
0
150
200
250
300
350
400
450
500
550
Wavelength /nm

(*b*)

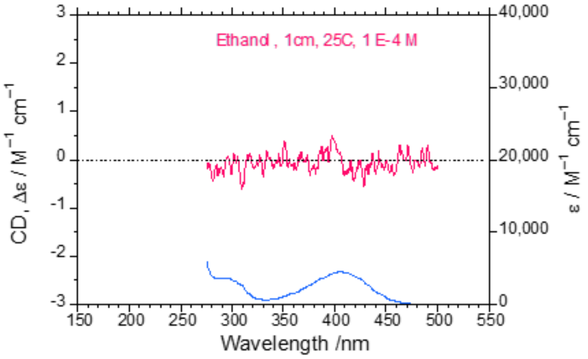
Ethanol , 1cm, 25C, 1 E-4 M
CD, Δε / M⁻¹ cm⁻¹
3
2
1
0
-1
-2
-3
ε / M⁻¹ cm⁻¹
40,000
30,000
20,000
10,000
0
150
200
250
300
350
400
450
500
550
Wavelength /nm

(*c*)

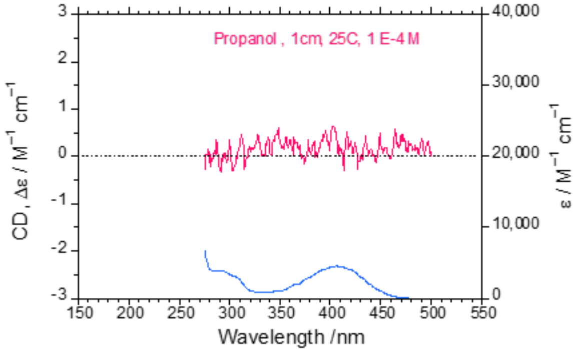
Propanol , 1cm, 25C, 1 E-4 M
CD, Δε / M⁻¹ cm⁻¹
3
2
1
0
-1
-2
-3
ε / M⁻¹ cm⁻¹
40,000
30,000
20,000
10,000
0
150
200
250
300
350
400
450
500
550
Wavelength /nm

(*d*)

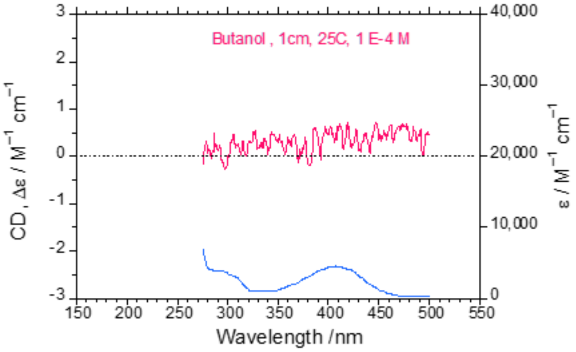
Butanol , 1cm, 25C, 1 E-4 M
CD, Δε / M⁻¹ cm⁻¹
3
2
1
0
-1
-2
-3
ε / M⁻¹ cm⁻¹
40,000
30,000
20,000
10,000
0
150
200
250
300
350
400
450
500
550
Wavelength /nm

(*e*)

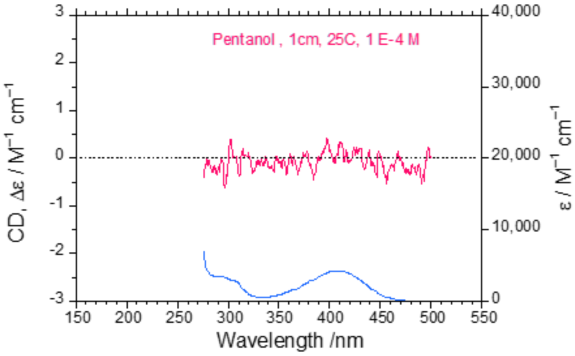
Pentanol , 1cm, 25C, 1 E-4 M
CD, Δε / M⁻¹ cm⁻¹
3
2
1
0
-1
-2
-3
ε / M⁻¹ cm⁻¹
40,000
30,000
20,000
10,000
0
150
200
250
300
350
400
450
500
550
Wavelength /nm

(*f*)

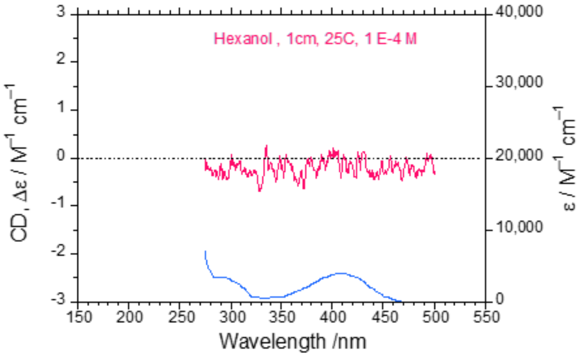
Hexanol , 1cm, 25C, 1 E-4 M
CD, Δε / M⁻¹ cm⁻¹
3
2
1
0
-1
-2
-3
ε / M⁻¹ cm⁻¹
40,000
30,000
20,000
10,000
0
150
200
250
300
350
400
450
500
550
Wavelength /nm

(*g*)

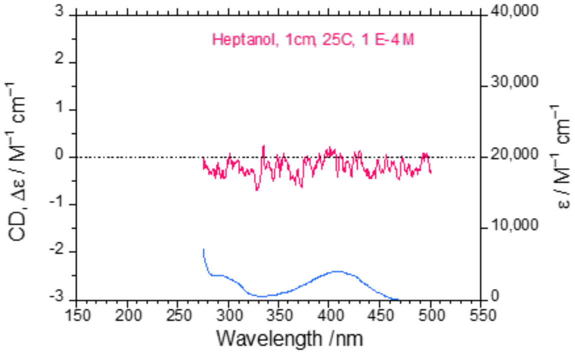
Heptanol, 1cm, 25C, 1 E-4 M
CD, Δε / M⁻¹ cm⁻¹
3
2
1
0
-1
-2
-3
ε / M⁻¹ cm⁻¹
40,000
30,000
20,000
10,000
0
150
200
250
300
350
400
450
500
550
Wavelength /nm

(*h*)

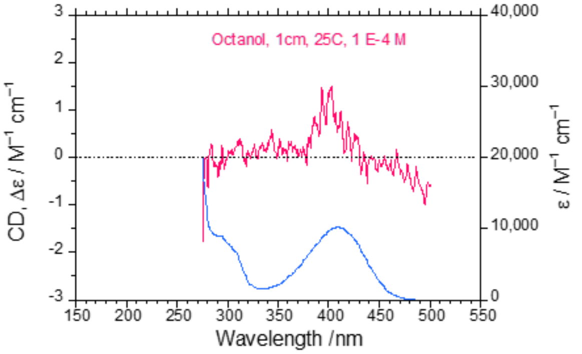
Octanol, 1cm, 25C, 1 E-4 M
CD, Δε / M⁻¹ cm⁻¹
3
2
1
0
-1
-2
-3
ε / M⁻¹ cm⁻¹
40,000
30,000
20,000
10,000
0
150
200
250
300
350
400
450
500
550
Wavelength /nm

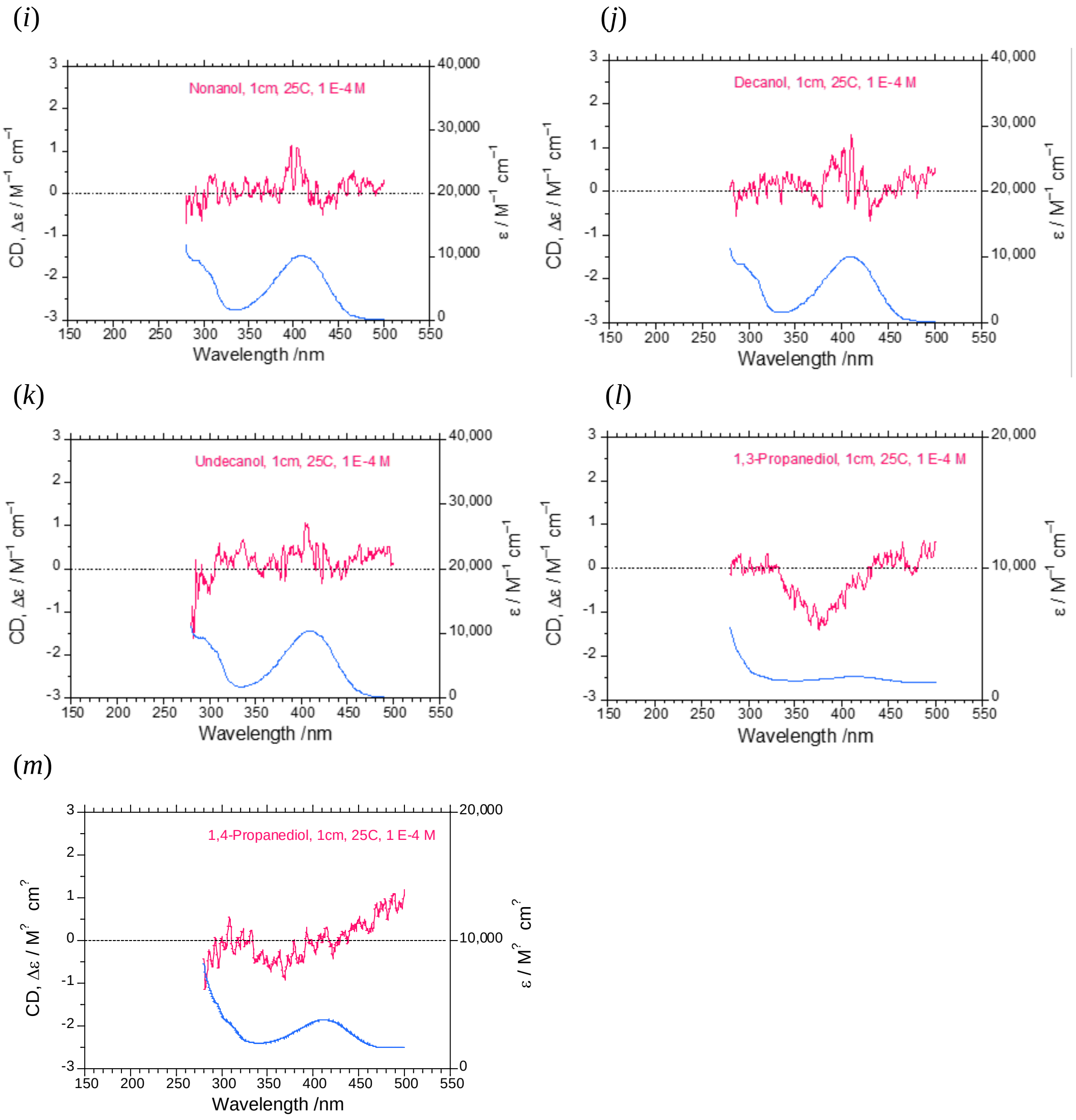

Fig. S4: CD spectra of **DSA** in Methanol (a), Ethanol (b), *n*-Propanol (c), *n*-Butanol (d), *n*-Pentanol (e), *n*-Hexanol (f), *n*-Heptanol (g), *n*-Octanol (h), *n*-Nonanol (i), *n*-Decanol (j), *n*-Undecanol (k), 1,3-Propanediol (l), 1,4-Butanediol (m).

(*a*)

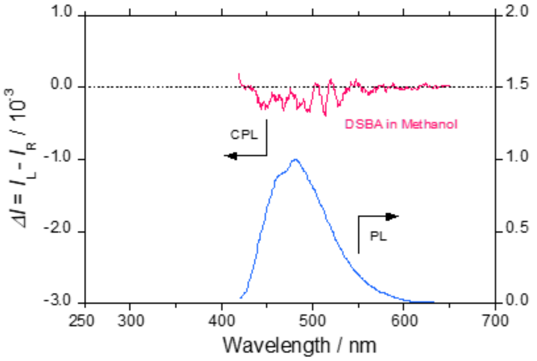
DSBA in Methanol
CPL
PL
$\Delta I = I_L - I_R$ / 10^{-3}
$I = (I_L + I_R)/2$
Wavelength / nm
1.0
0.0
-1.0
-2.0
-3.0
2.0
1.5
1.0
0.5
0.0
250
300
400
500
600
700

(*b*)

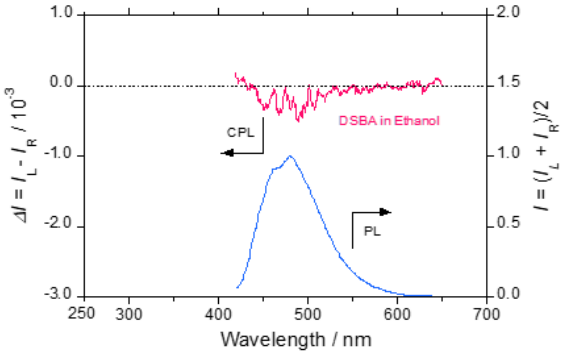
DSBA in Ethanol
CPL
PL
$\Delta I = I_L - I_R$ / 10^{-3}
$I = (I_L + I_R)/2$
Wavelength / nm
1.0
0.0
-1.0
-2.0
-3.0
2.0
1.5
1.0
0.5
0.0
250
300
400
500
600
700

(*c*)

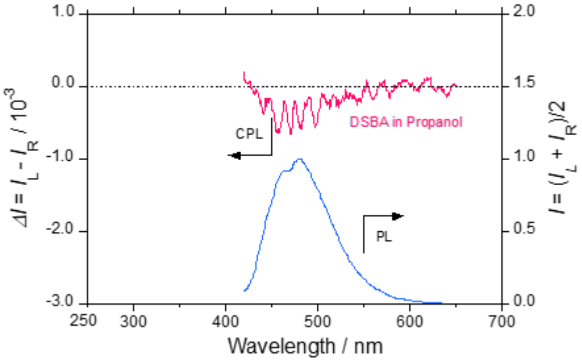
DSBA in Propanol
CPL
PL
$\Delta I = I_L - I_R$ / 10^{-3}
$I = (I_L + I_R)/2$
Wavelength / nm
1.0
0.0
-1.0
-2.0
-3.0
2.0
1.5
1.0
0.5
0.0
250
300
400
500
600
700

(*d*)

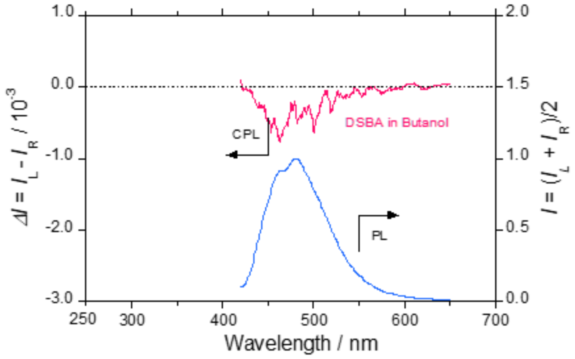
DSBA in Butanol
CPL
PL
$\Delta I = I_L - I_R$ / 10^{-3}
$I = (I_L + I_R)/2$
Wavelength / nm
1.0
0.0
-1.0
-2.0
-3.0
2.0
1.5
1.0
0.5
0.0
250
300
400
500
600
700

(*e*)

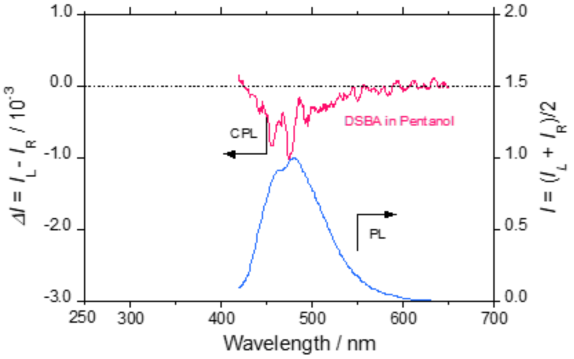
DSBA in Pentanol
CPL
PL
$\Delta I = I_L - I_R$ / 10^{-3}
$I = (I_L + I_R)/2$
Wavelength / nm
1.0
0.0
-1.0
-2.0
-3.0
2.0
1.5
1.0
0.5
0.0
250
300
400
500
600
700

(*f*)

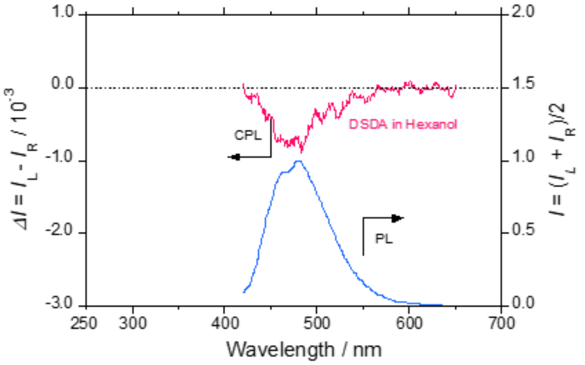
DSDA in Hexanol
CPL
PL
$\Delta I = I_L - I_R$ / 10^{-3}
$I = (I_L + I_R)/2$
Wavelength / nm
1.0
0.0
-1.0
-2.0
-3.0
2.0
1.5
1.0
0.5
0.0
250
300
400
500
600
700

(*g*)

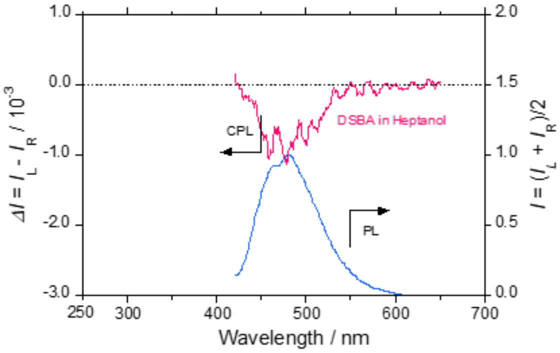
DSBA in Heptanol
CPL
PL
$\Delta I = I_L - I_R$ / 10^{-3}
$I = (I_L + I_R)/2$
Wavelength / nm
1.0
0.0
-1.0
-2.0
-3.0
2.0
1.5
1.0
0.5
0.0
250
300
400
500
600
700

(*h*)

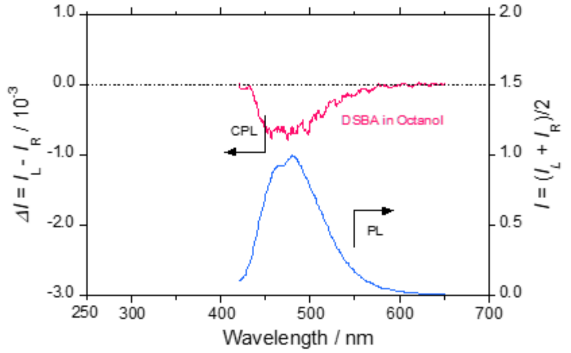
DSBA in Octanol
CPL
PL
$\Delta I = I_L - I_R$ / 10^{-3}
$I = (I_L + I_R)/2$
Wavelength / nm
1.0
0.0
-1.0
-2.0
-3.0
2.0
1.5
1.0
0.5
0.0
250
300
400
500
600
700

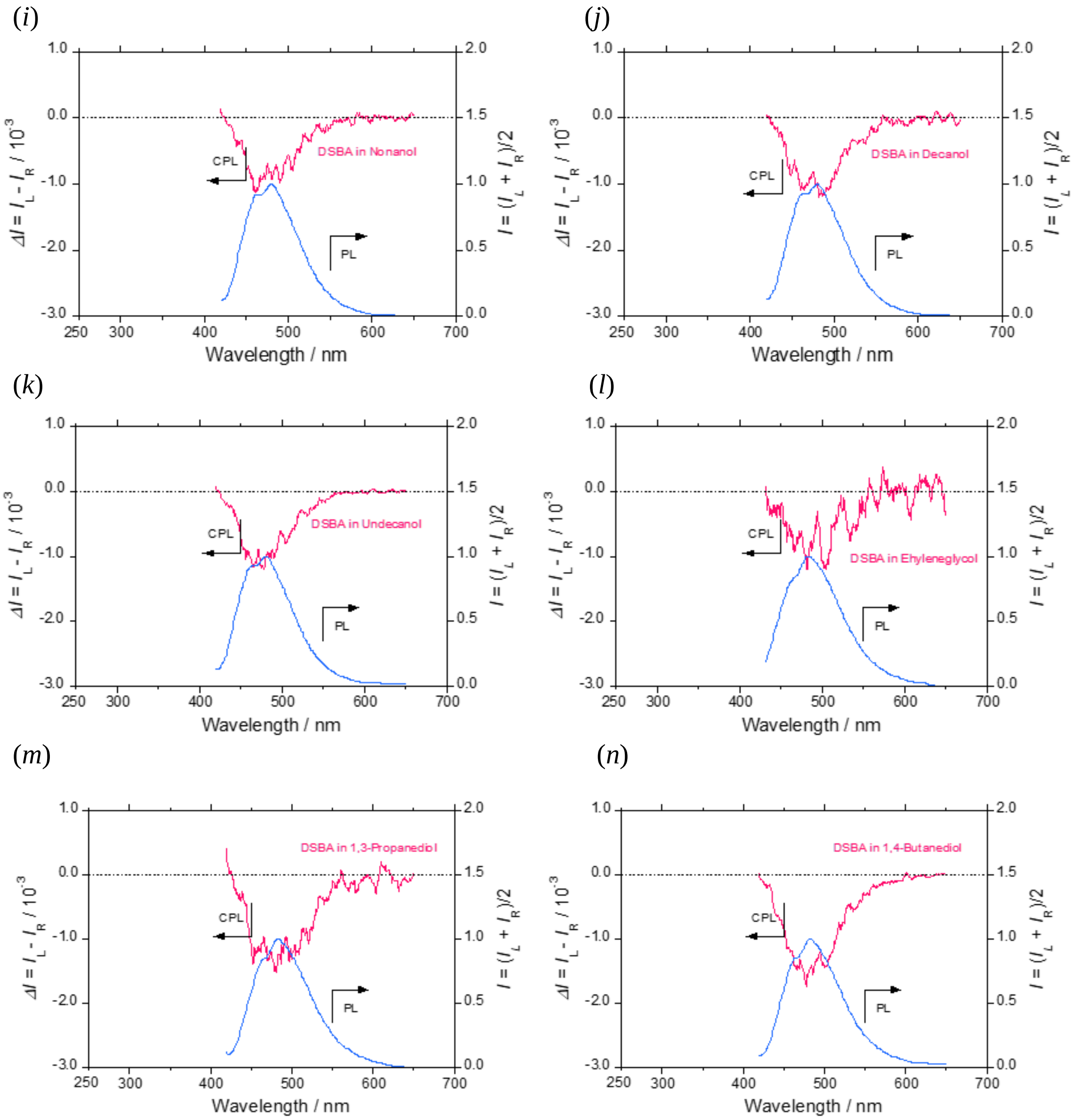

Fig. S5: CPL spectra of **DSBA** in Methanol (a), Ethanol (b), *n*-Propanol (c), *n*-Butanol (d), *n*-Pentanol e), *n*-Hexanol (f), *n*-Heptanol (g), *n*-Octanol (h), *n*-Nonanol (i), *n*-Decanol (j), *n*-Undecanol (k), Ethyleneglycol (l), 1,3-Propanediol (m), 1,4-Butanediol (n).

(*a*)

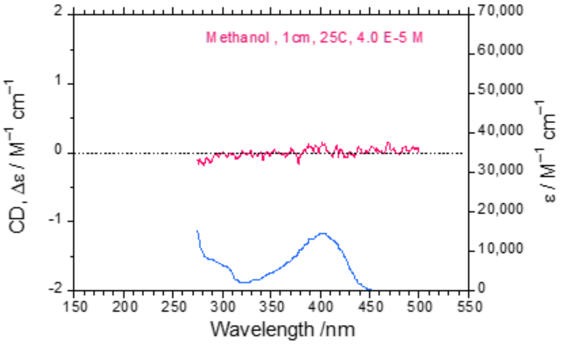
Methanol , 1cm, 25C, 4.0 E-5 M
CD, Δε / M^{-1} cm^{-1}
ε / M^{-1} cm^{-1}
Wavelength /nm
2
1
0
-1
-2
70,000
60,000
50,000
40,000
30,000
20,000
10,000
0
150
200
250
300
350
400
450
500
550

(*b*)

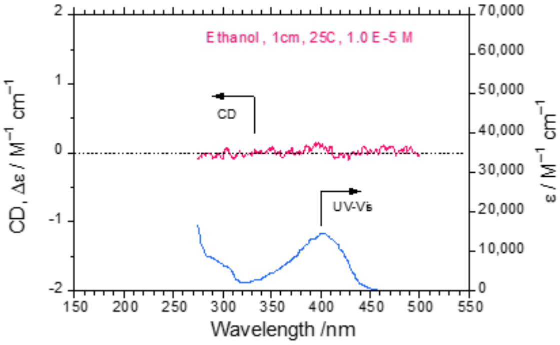
Ethanol , 1cm, 25C, 1.0 E-5 M
CD
UV-Vis
CD, Δε / M^{-1} cm^{-1}
ε / M^{-1} cm^{-1}
Wavelength /nm
2
1
0
-1
-2
70,000
60,000
50,000
40,000
30,000
20,000
10,000
0
150
200
250
300
350
400
450
500
550

(*c*)

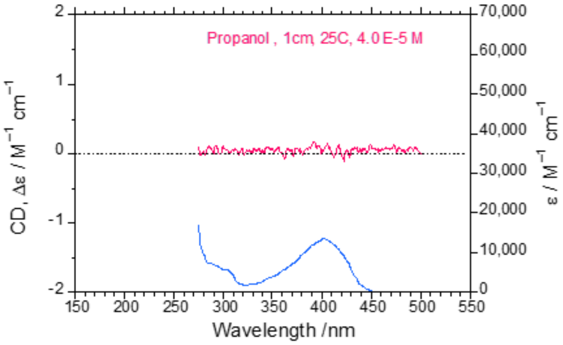
Propanol , 1cm, 25C, 4.0 E-5 M
CD, Δε / M^{-1} cm^{-1}
ε / M^{-1} cm^{-1}
Wavelength /nm
2
1
0
-1
-2
70,000
60,000
50,000
40,000
30,000
20,000
10,000
0
150
200
250
300
350
400
450
500
550

(*d*)

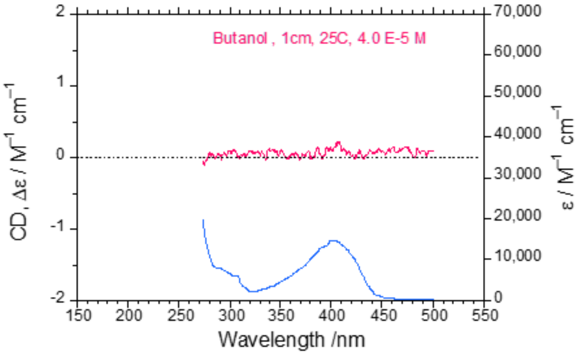
Butanol , 1cm, 25C, 4.0 E-5 M
CD, Δε / M^{-1} cm^{-1}
ε / M^{-1} cm^{-1}
Wavelength /nm
2
1
0
-1
-2
70,000
60,000
50,000
40,000
30,000
20,000
10,000
0
150
200
250
300
350
400
450
500
550

(*e*)

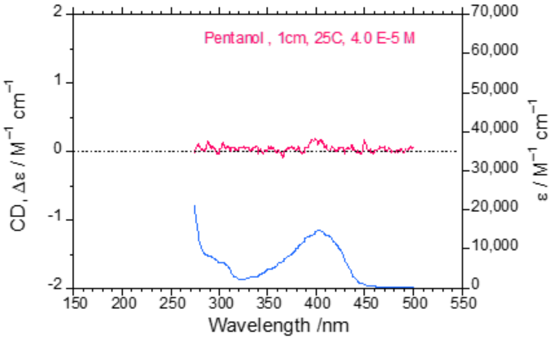
Pentanol , 1cm, 25C, 4.0 E-5 M
CD, Δε / M^{-1} cm^{-1}
ε / M^{-1} cm^{-1}
Wavelength /nm
2
1
0
-1
-2
70,000
60,000
50,000
40,000
30,000
20,000
10,000
0
150
200
250
300
350
400
450
500
550

(*f*)

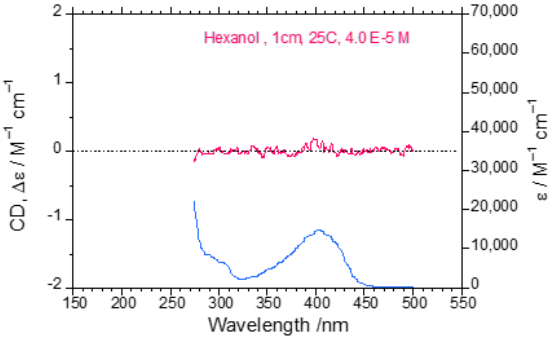
Hexanol , 1cm, 25C, 4.0 E-5 M
CD, Δε / M^{-1} cm^{-1}
ε / M^{-1} cm^{-1}
Wavelength /nm
2
1
0
-1
-2
70,000
60,000
50,000
40,000
30,000
20,000
10,000
0
150
200
250
300
350
400
450
500
550

(*g*)

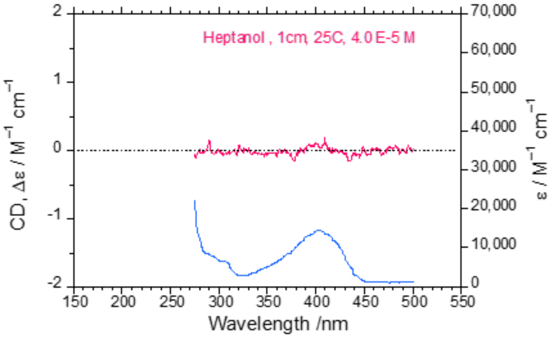
Heptanol , 1cm, 25C, 4.0 E-5 M
CD, Δε / M^{-1} cm^{-1}
ε / M^{-1} cm^{-1}
Wavelength /nm
2
1
0
-1
-2
70,000
60,000
50,000
40,000
30,000
20,000
10,000
0
150
200
250
300
350
400
450
500
550

(*h*)

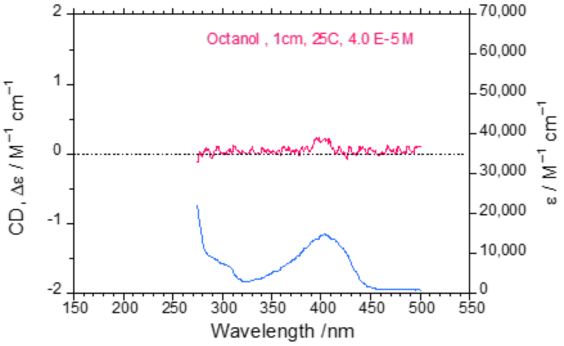
Octanol , 1cm, 25C, 4.0 E-5 M
CD, Δε / M^{-1} cm^{-1}
ε / M^{-1} cm^{-1}
Wavelength /nm
2
1
0
-1
-2
70,000
60,000
50,000
40,000
30,000
20,000
10,000
0
150
200
250
300
350
400
450
500
550

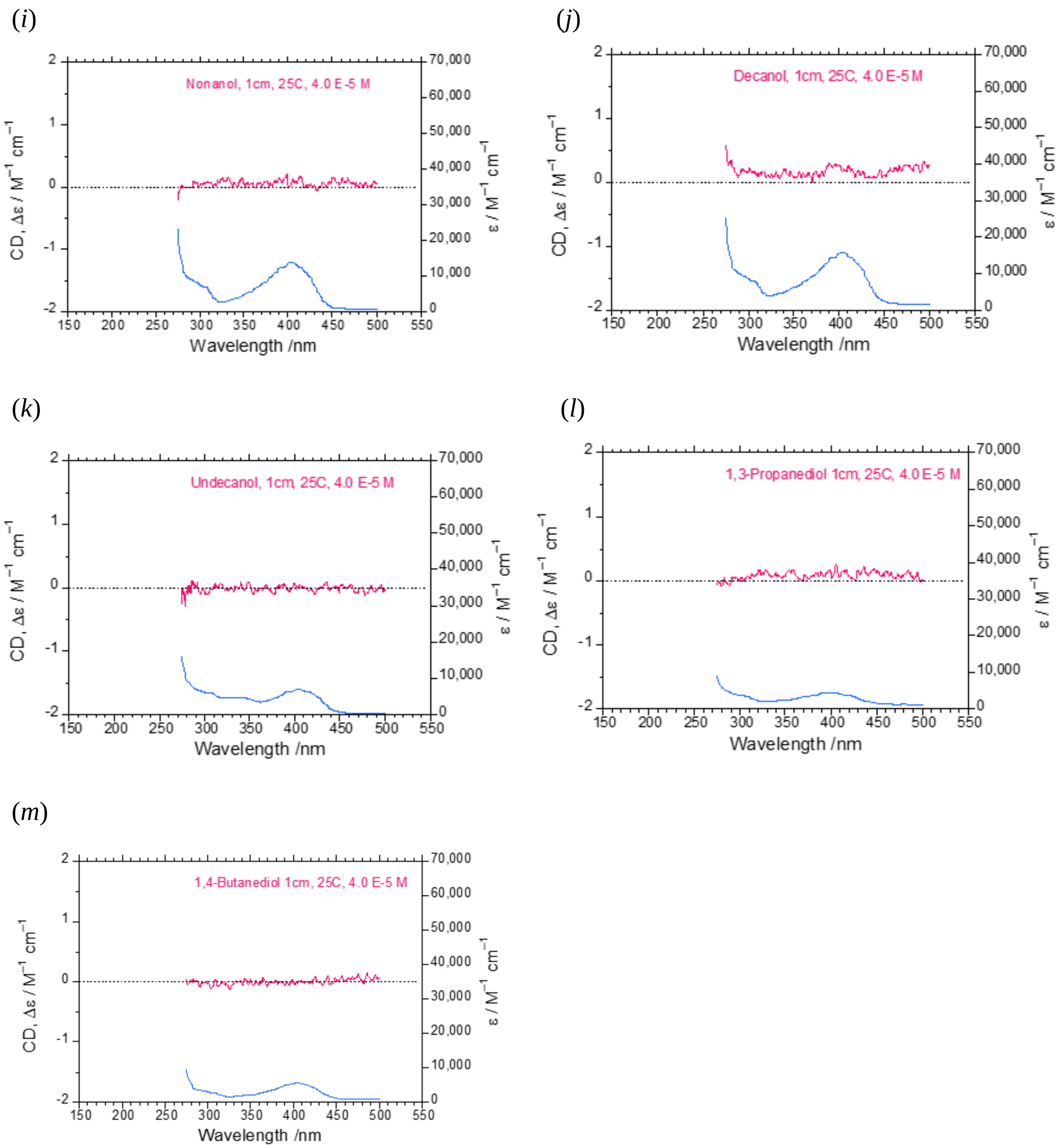

Fig. S6: CD spectra of **DSBA** in Methanol (a), Ethanol (b), *n*-Propanol (c), *n*-Butanol (d), *n*-Pentanol (e), *n*-Hexanol (f), *n*-Heptanol (g), *n*-Octanol (h), *n*-Nonanol (i), *n*-Decanol (j), *n*-Undecanol (k), 1,3-Propanediol (l), 1,4-Butanediol (m).

(*a*)

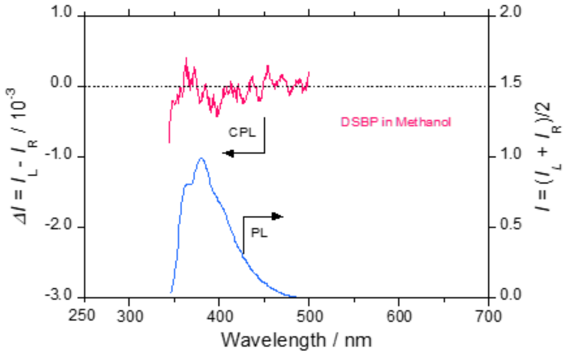
$\Delta I = I_L - I_R$ / 10^{-3}
1.0
0.0
-1.0
-2.0
-3.0
$I = (I_L + I_R)/2$
2.0
1.5
1.0
0.5
0.0
250
300
400
500
600
700
Wavelength / nm
CPL
PL
DSBP in Methanol

(*b*)

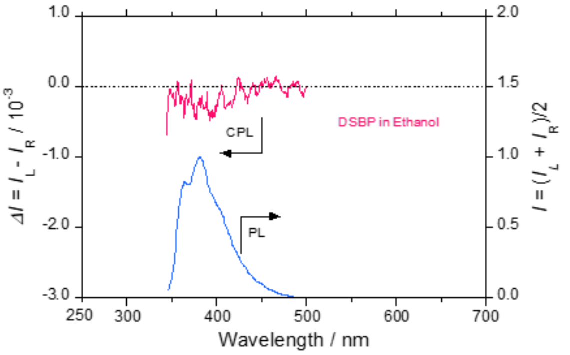
$\Delta I = I_L - I_R$ / 10^{-3}
1.0
0.0
-1.0
-2.0
-3.0
$I = (I_L + I_R)/2$
2.0
1.5
1.0
0.5
0.0
250
300
400
500
600
700
Wavelength / nm
CPL
PL
DSBP in Ethanol

(*c*)

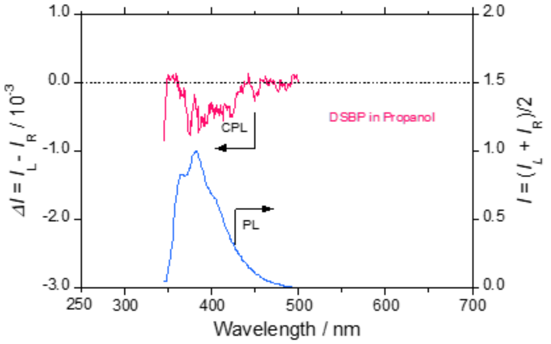
$\Delta I = I_L - I_R$ / 10^{-3}
1.0
0.0
-1.0
-2.0
-3.0
$I = (I_L + I_R)/2$
2.0
1.5
1.0
0.5
0.0
250
300
400
500
600
700
Wavelength / nm
CPL
PL
DSBP in Propanol

(*d*)

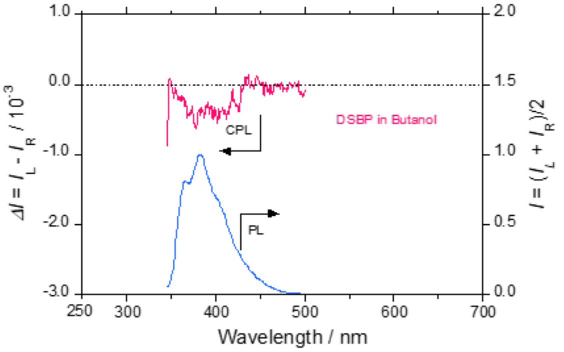
$\Delta I = I_L - I_R$ / 10^{-3}
1.0
0.0
-1.0
-2.0
-3.0
$I = (I_L + I_R)/2$
2.0
1.5
1.0
0.5
0.0
250
300
400
500
600
700
Wavelength / nm
CPL
PL
DSBP in Butanol

(*e*)

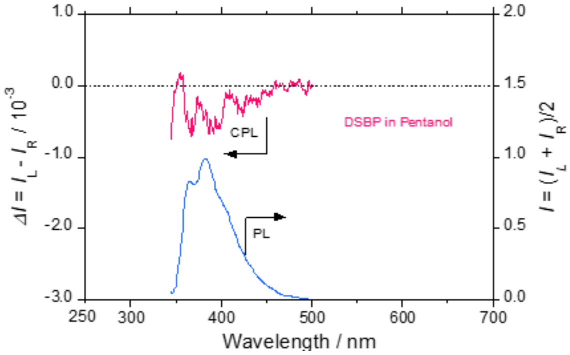
$\Delta I = I_L - I_R$ / 10^{-3}
1.0
0.0
-1.0
-2.0
-3.0
$I = (I_L + I_R)/2$
2.0
1.5
1.0
0.5
0.0
250
300
400
500
600
700
Wavelength / nm
CPL
PL
DSBP in Pentanol

(*f*)

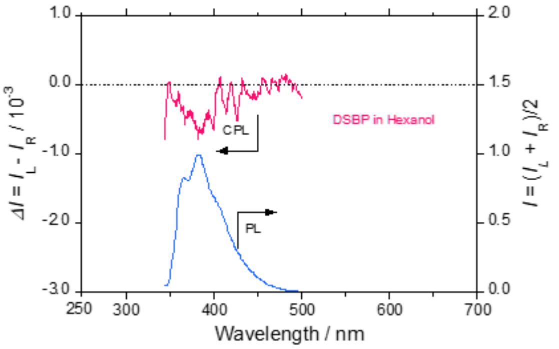
$\Delta I = I_L - I_R$ / 10^{-3}
1.0
0.0
-1.0
-2.0
-3.0
$I = (I_L + I_R)/2$
2.0
1.5
1.0
0.5
0.0
250
300
400
500
600
700
Wavelength / nm
CPL
PL
DSBP in Hexanol

(*g*)

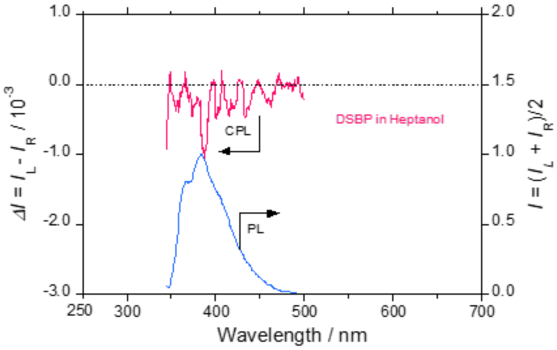
$\Delta I = I_L - I_R$ / 10^{-3}
1.0
0.0
-1.0
-2.0
-3.0
$I = (I_L + I_R)/2$
2.0
1.5
1.0
0.5
0.0
250
300
400
500
600
700
Wavelength / nm
CPL
PL
DSBP in Heptanol

(*h*)

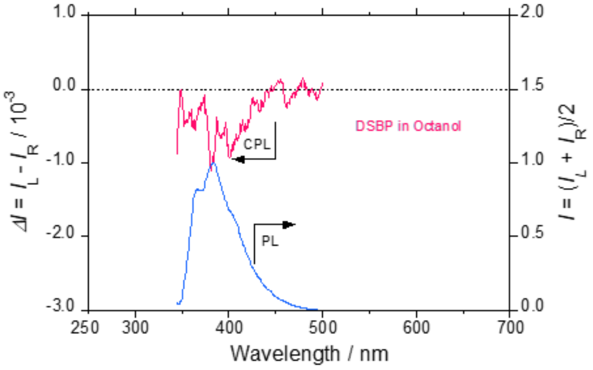
$\Delta I = I_L - I_R$ / 10^{-3}
1.0
0.0
-1.0
-2.0
-3.0
$I = (I_L + I_R)/2$
2.0
1.5
1.0
0.5
0.0
250
300
400
500
600
700
Wavelength / nm
CPL
PL
DSBP in Octanol

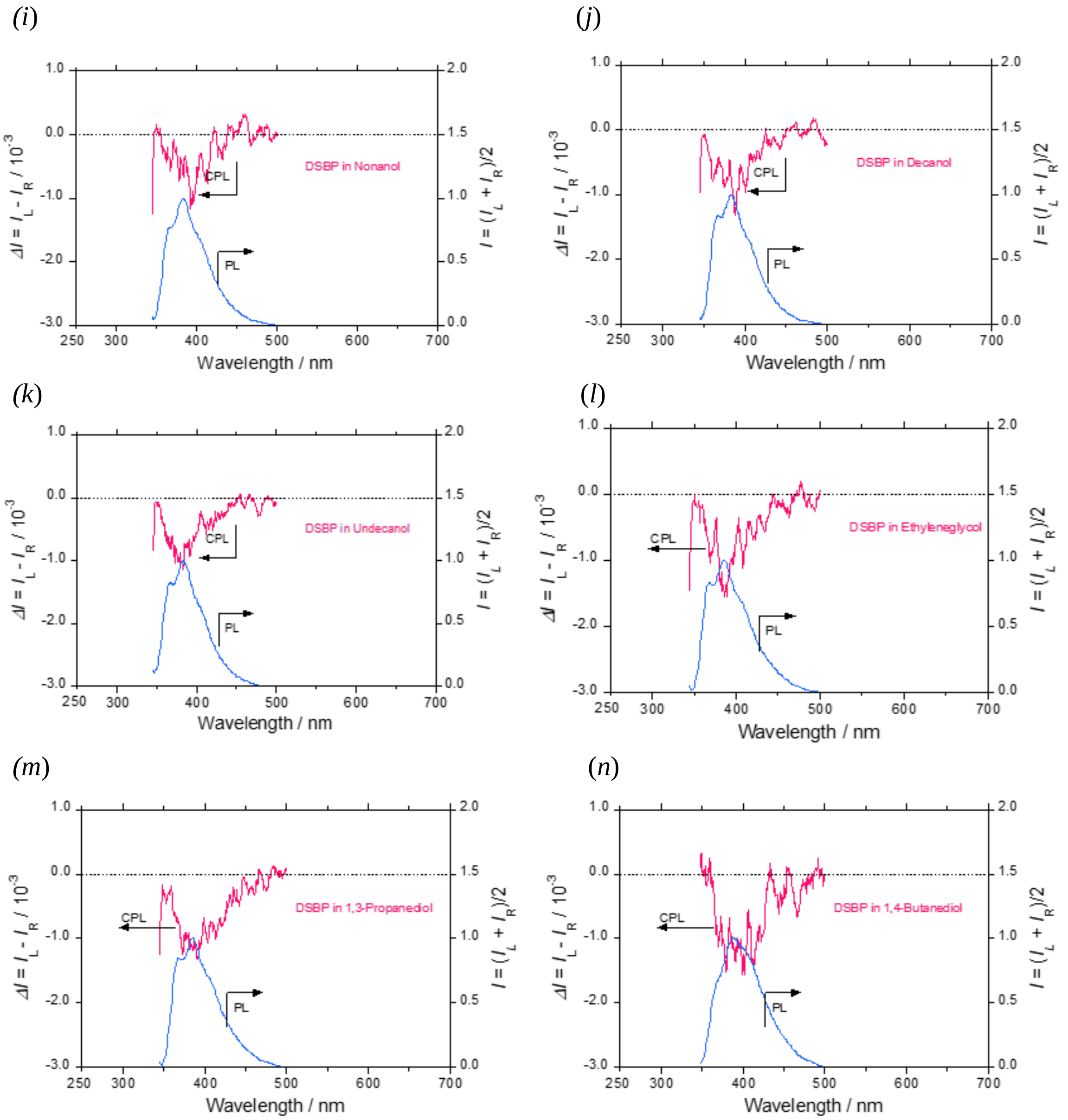

Fig. S7: CPL spectra of **DSBP** in Methanol ol (a), Ethanol (b), *n*-Propanol (c), *n*-Butanol (d), *n*-Pentanol e), *n*-Hexanol (f), *n*-Heptanol (g), *n*-Octanol (h), *n*-Nonanol (i), *n*-Decanol (j), *n*-Undecanol (k), Ethyleneglycol (l), 1,3-Propanediol (m), 1,4-Butanediol (n).

(*a*)

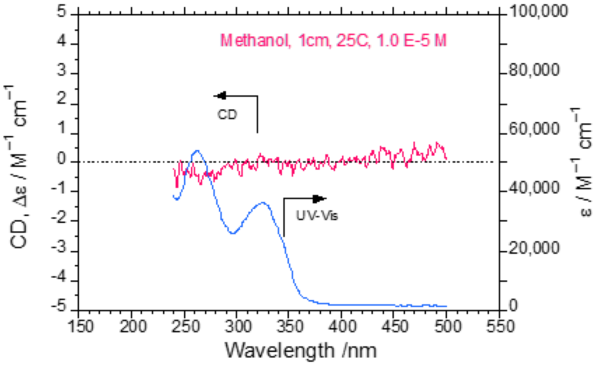
Methanol, 1cm, 25C, 1.0 E-5 M
CD
UV-Vis
CD, Δε / M^{-1} cm^{-1}
ε / M^{-1} cm^{-1}
Wavelength /nm
5
4
3
2
1
0
-1
-2
-3
-4
-5
100,000
80,000
60,000
40,000
20,000
0
150
200
250
300
350
400
450
500
550

(*b*)

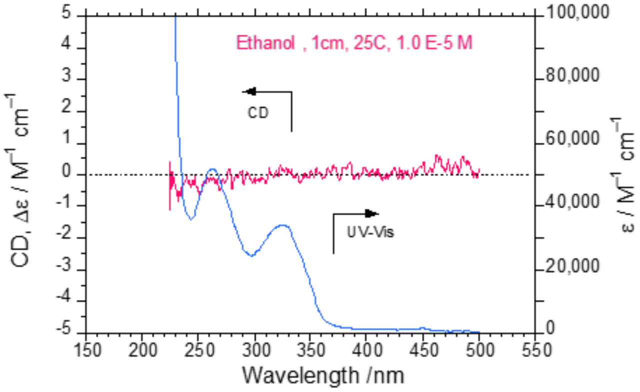
Ethanol , 1cm, 25C, 1.0 E-5 M
CD
UV-Vis
CD, Δε / M^{-1} cm^{-1}
ε / M^{-1} cm^{-1}
Wavelength /nm
5
4
3
2
1
0
-1
-2
-3
-4
-5
100,000
80,000
60,000
40,000
20,000
0
150
200
250
300
350
400
450
500
550

(*c*)

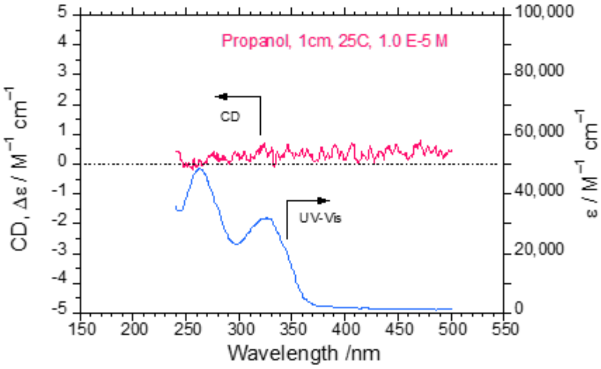
Propanol, 1cm, 25C, 1.0 E-5 M
CD
UV-Vis
CD, Δε / M^{-1} cm^{-1}
ε / M^{-1} cm^{-1}
Wavelength /nm
5
4
3
2
1
0
-1
-2
-3
-4
-5
100,000
80,000
60,000
40,000
20,000
0
150
200
250
300
350
400
450
500
550

(*d*)

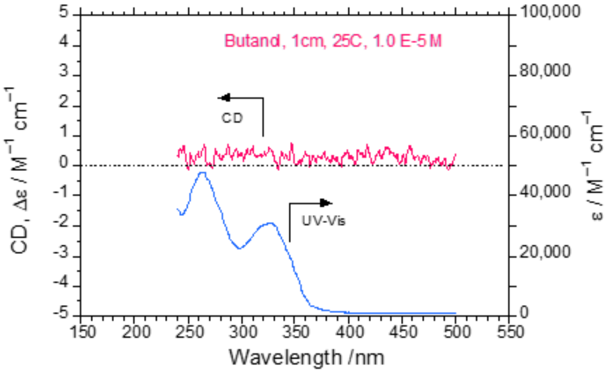
Butanol, 1cm, 25C, 1.0 E-5 M
CD
UV-Vis
CD, Δε / M^{-1} cm^{-1}
ε / M^{-1} cm^{-1}
Wavelength /nm
5
4
3
2
1
0
-1
-2
-3
-4
-5
100,000
80,000
60,000
40,000
20,000
0
150
200
250
300
350
400
450
500
550

(*e*)

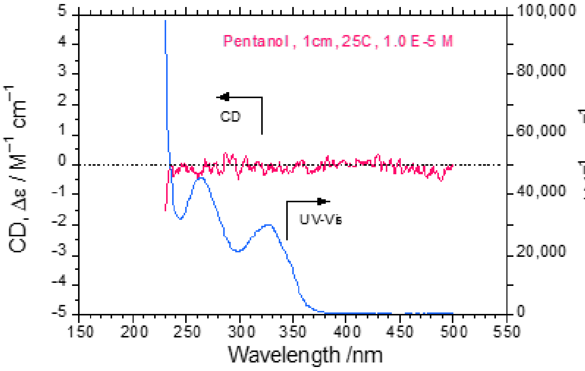
Pentanol , 1cm, 25C , 1.0 E-5 M
CD
UV-Vis
CD, Δε / M^{-1} cm^{-1}
ε / M^{-1} cm^{-1}
Wavelength /nm
5
4
3
2
1
0
-1
-2
-3
-4
-5
100,000
80,000
60,000
40,000
20,000
0
150
200
250
300
350
400
450
500
550

(*f*)

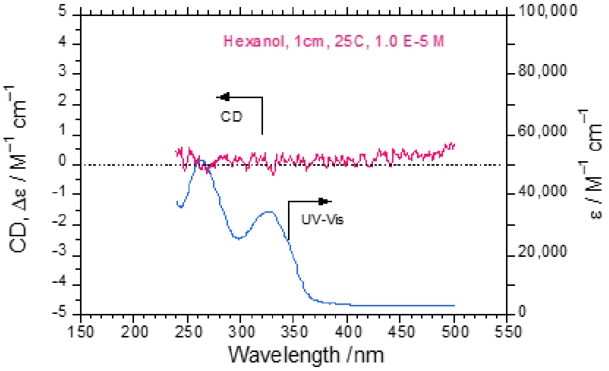
Hexanol, 1cm, 25C, 1.0 E-5 M
CD
UV-Vis
CD, Δε / M^{-1} cm^{-1}
ε / M^{-1} cm^{-1}
Wavelength /nm
5
4
3
2
1
0
-1
-2
-3
-4
-5
100,000
80,000
60,000
40,000
20,000
0
150
200
250
300
350
400
450
500
550

(*g*)

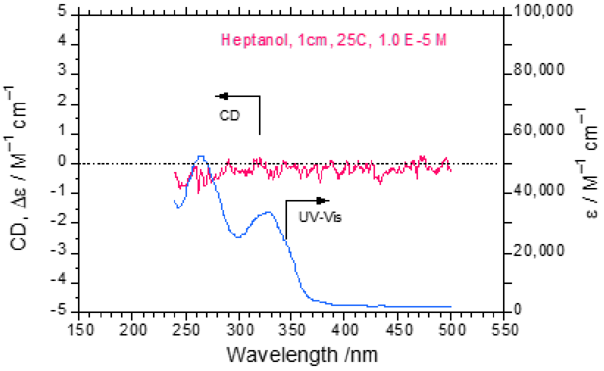
Heptanol, 1cm, 25C, 1.0 E-5 M
CD
UV-Vis
CD, Δε / M^{-1} cm^{-1}
ε / M^{-1} cm^{-1}
Wavelength /nm
5
4
3
2
1
0
-1
-2
-3
-4
-5
100,000
80,000
60,000
40,000
20,000
0
150
200
250
300
350
400
450
500
550

(*h*)

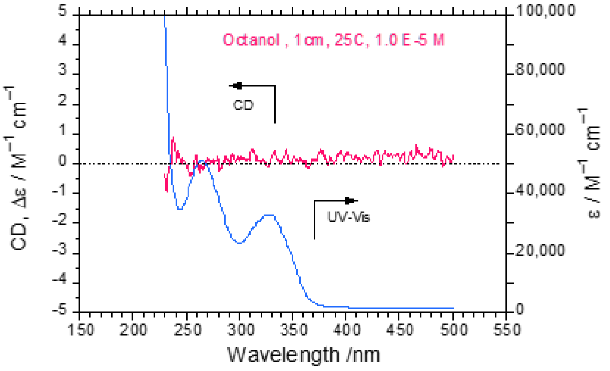
Octanol , 1cm, 25C, 1.0 E-5 M
CD
UV-Vis
CD, Δε / M^{-1} cm^{-1}
ε / M^{-1} cm^{-1}
Wavelength /nm
5
4
3
2
1
0
-1
-2
-3
-4
-5
100,000
80,000
60,000
40,000
20,000
0
150
200
250
300
350
400
450
500
550

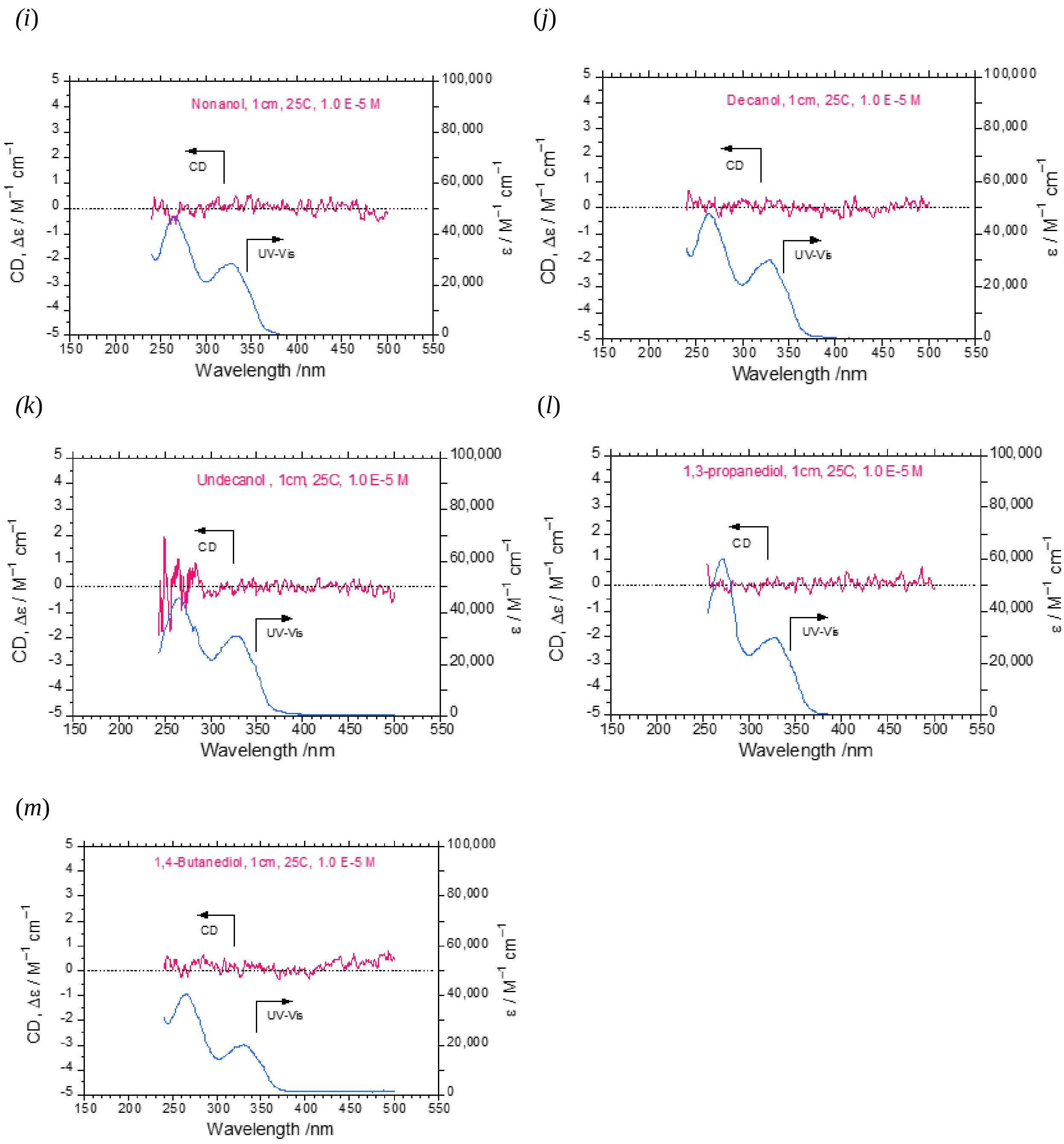

Fig. S8: CD spectra of **DSBP** in Methanol (a), Ethanol (b), *n*-Propanol (c), *n*-Butanol (d), *n*-Pentanol (e), *n*-Hexanol (f), *n*-Heptanol (g), *n*-Octanol (h), *n*-Nonanol (i), *n*-Decanol (j), *n*-Undecanol (k), 1,3-Propanediol (l), 1,4-Butanediol (m).

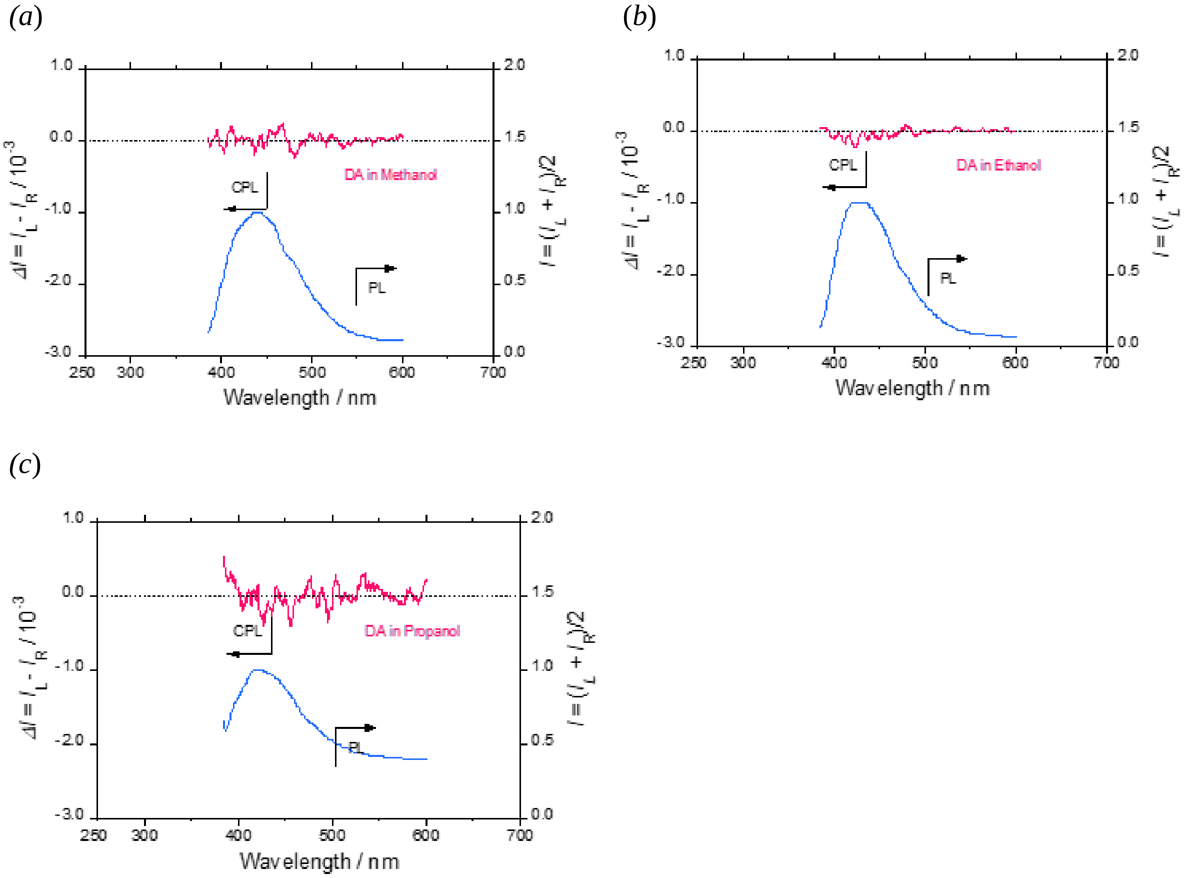

Fig. S9: CPL spectra of **BA** in Methanol (a), Ethanol (b), *n*-Propanol (c).

(*a*)

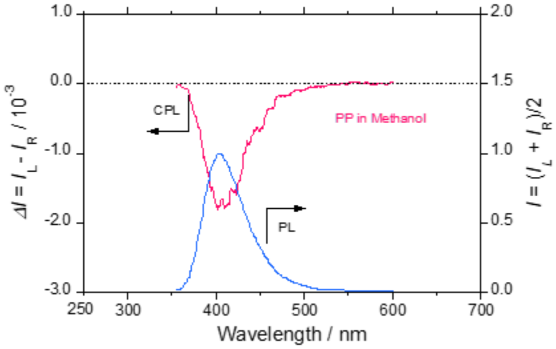
1.0
0.0
-1.0
-2.0
-3.0
2.0
1.5
1.0
0.5
0.0
250
300
400
500
600
700
$\Delta I = I_L - I_R$ / 10^{-3}
$I = (I_L + I_R)/2$
Wavelength / nm
CPL
PL
PP in Methanol

(*b*)

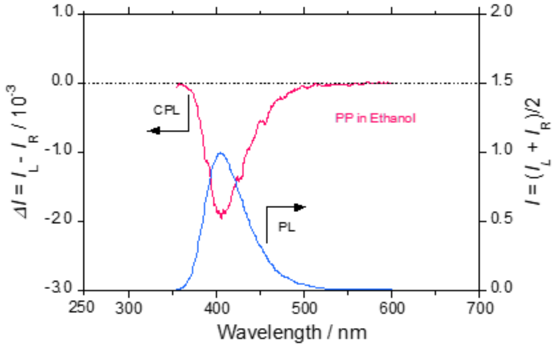
1.0
0.0
-1.0
-2.0
-3.0
2.0
1.5
1.0
0.5
0.0
250
300
400
500
600
700
$\Delta I = I_L - I_R$ / 10^{-3}
$I = (I_L + I_R)/2$
Wavelength / nm
CPL
PL
PP in Ethanol

(*c*)

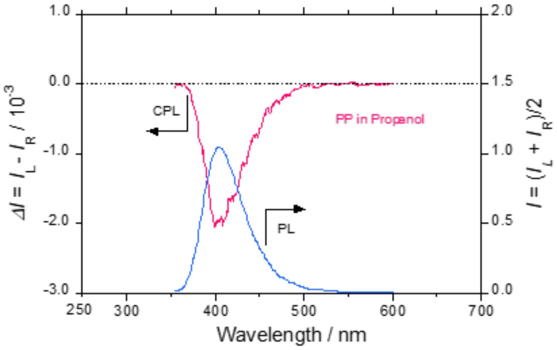
1.0
0.0
-1.0
-2.0
-3.0
2.0
1.5
1.0
0.5
0.0
250
300
400
500
600
700
$\Delta I = I_L - I_R$ / 10^{-3}
$I = (I_L + I_R)/2$
Wavelength / nm
CPL
PL
PP in Propanol

(*d*)

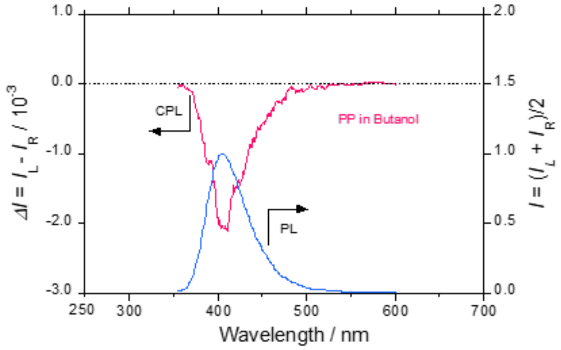
1.0
0.0
-1.0
-2.0
-3.0
2.0
1.5
1.0
0.5
0.0
250
300
400
500
600
700
$\Delta I = I_L - I_R$ / 10^{-3}
$I = (I_L + I_R)/2$
Wavelength / nm
CPL
PL
PP in Butanol

(*e*)

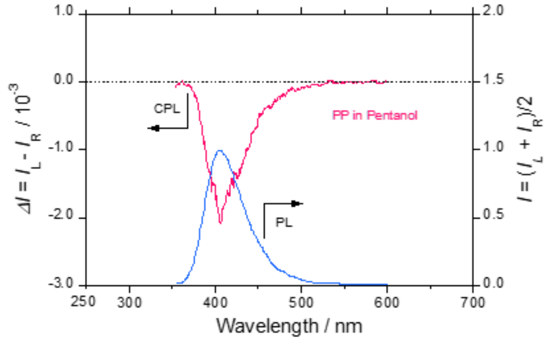
1.0
0.0
-1.0
-2.0
-3.0
2.0
1.5
1.0
0.5
0.0
250
300
400
500
600
700
$\Delta I = I_L - I_R$ / 10^{-3}
$I = (I_L + I_R)/2$
Wavelength / nm
CPL
PL
PP in Pentanol

(*f*)

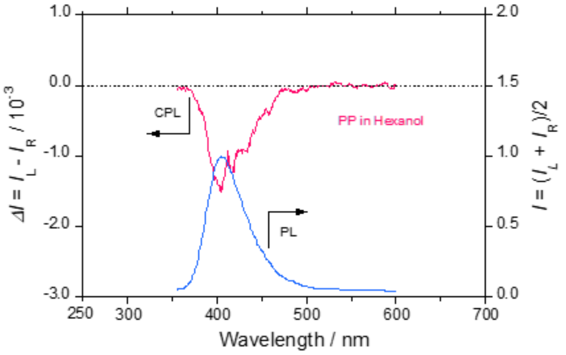
1.0
0.0
-1.0
-2.0
-3.0
2.0
1.5
1.0
0.5
0.0
250
300
400
500
600
700
$\Delta I = I_L - I_R$ / 10^{-3}
$I = (I_L + I_R)/2$
Wavelength / nm
CPL
PL
PP in Hexanol

(*g*)

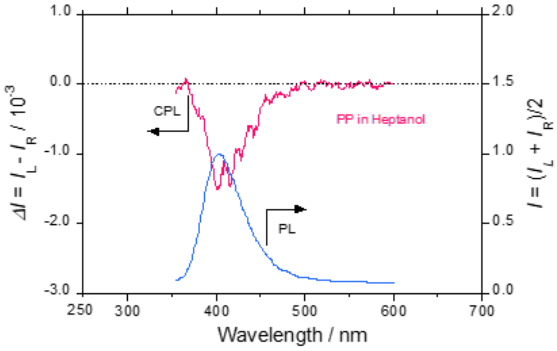
1.0
0.0
-1.0
-2.0
-3.0
2.0
1.5
1.0
0.5
0.0
250
300
400
500
600
700
$\Delta I = I_L - I_R$ / 10^{-3}
$I = (I_L + I_R)/2$
Wavelength / nm
CPL
PL
PP in Heptanol

(*h*)

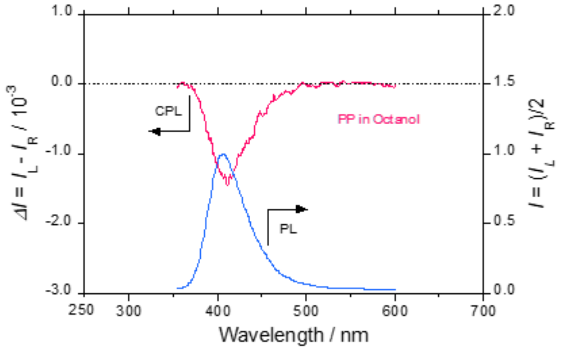
1.0
0.0
-1.0
-2.0
-3.0
2.0
1.5
1.0
0.5
0.0
250
300
400
500
600
700
$\Delta I = I_L - I_R$ / 10^{-3}
$I = (I_L + I_R)/2$
Wavelength / nm
CPL
PL
PP in Octanol

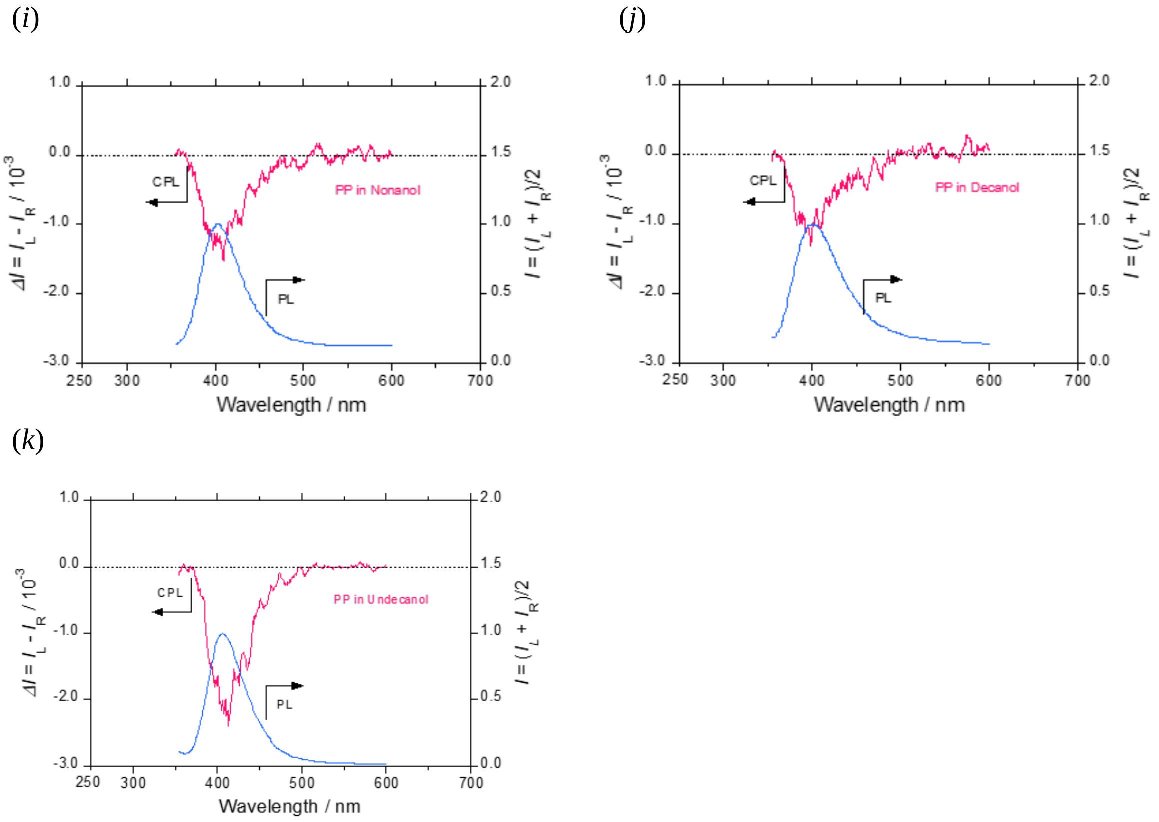

Fig. S10: CPL spectra of **PP** in Methanol ol (a), Ethanol (b), *n*-Propanol (c), *n*-Butanol (d), *n*-Pentanol e), *n*-Hexanol (f), *n*-Heptanol (g), *n*-Octanol (h), *n*-Nonanol (i), *n*-Decanol (j), *n*-Undecanol (k).

(*a*)

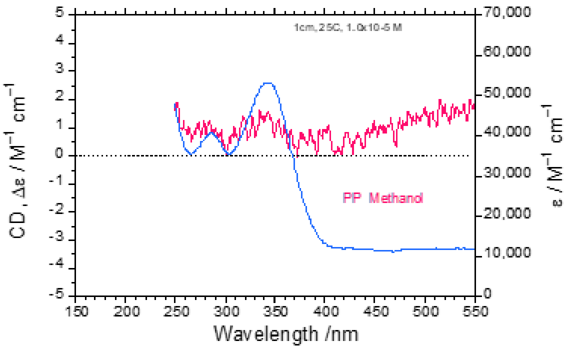
1cm, 25C, 1.0x10-5 M
PP Methanol
CD, Δε / M⁻¹ cm⁻¹
ε / M⁻¹ cm⁻¹
Wavelength /nm
5
4
3
2
1
0
-1
-2
-3
-4
-5
70,000
60,000
50,000
40,000
30,000
20,000
10,000
0
150
200
250
300
350
400
450
500
550

(*b*)

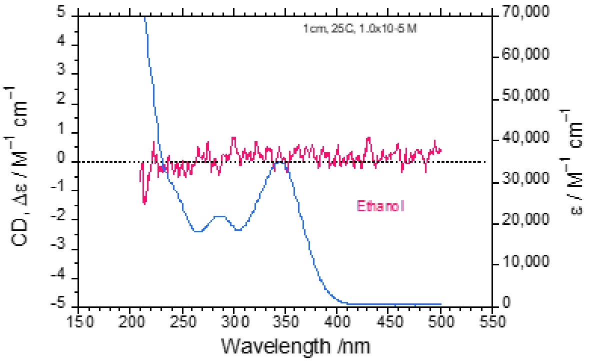
1cm, 25C, 1.0x10-5 M
Ethanol
CD, Δε / M⁻¹ cm⁻¹
ε / M⁻¹ cm⁻¹
Wavelength /nm
5
4
3
2
1
0
-1
-2
-3
-4
-5
70,000
60,000
50,000
40,000
30,000
20,000
10,000
0
150
200
250
300
350
400
450
500
550

(*c*)

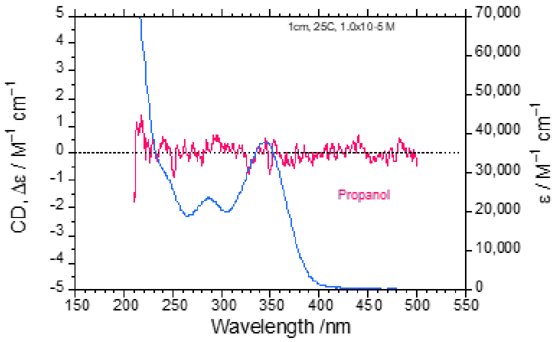
1cm, 25C, 1.0x10-5 M
Propanol
CD, Δε / M⁻¹ cm⁻¹
ε / M⁻¹ cm⁻¹
Wavelength /nm
5
4
3
2
1
0
-1
-2
-3
-4
-5
70,000
60,000
50,000
40,000
30,000
20,000
10,000
0
150
200
250
300
350
400
450
500
550

(*d*)

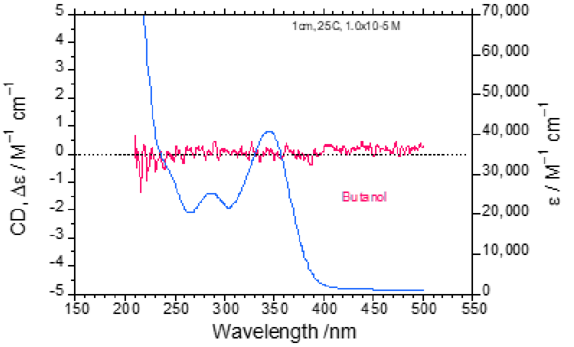
1cm, 25C, 1.0x10-5 M
Butanol
CD, Δε / M⁻¹ cm⁻¹
ε / M⁻¹ cm⁻¹
Wavelength /nm
5
4
3
2
1
0
-1
-2
-3
-4
-5
70,000
60,000
50,000
40,000
30,000
20,000
10,000
0
150
200
250
300
350
400
450
500
550

(*e*)

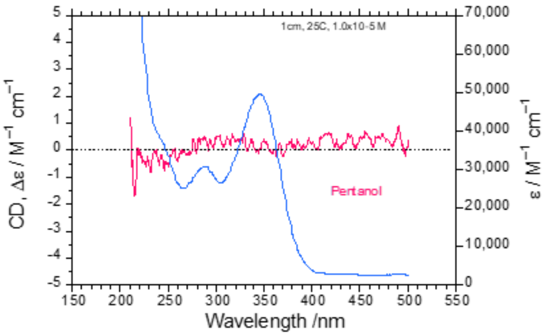
1cm, 25C, 1.0x10-5 M
Pentanol
CD, Δε / M⁻¹ cm⁻¹
ε / M⁻¹ cm⁻¹
Wavelength /nm
5
4
3
2
1
0
-1
-2
-3
-4
-5
70,000
60,000
50,000
40,000
30,000
20,000
10,000
0
150
200
250
300
350
400
450
500
550

(*f*)

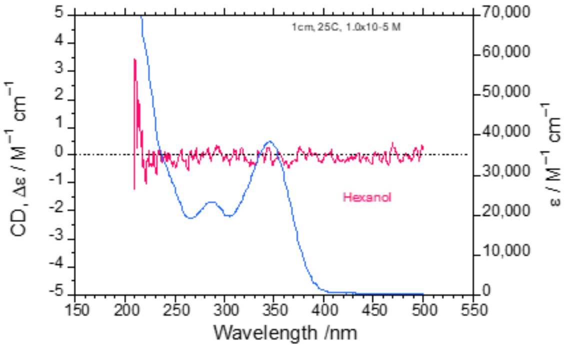
1cm, 25C, 1.0x10-5 M
Hexanol
CD, Δε / M⁻¹ cm⁻¹
ε / M⁻¹ cm⁻¹
Wavelength /nm
5
4
3
2
1
0
-1
-2
-3
-4
-5
70,000
60,000
50,000
40,000
30,000
20,000
10,000
0
150
200
250
300
350
400
450
500
550

(*g*)

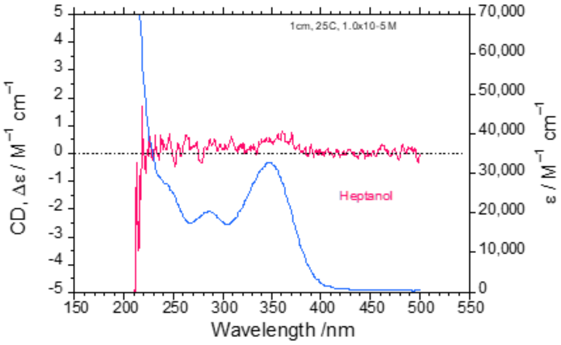
1cm, 25C, 1.0x10-5 M
Heptanol
CD, Δε / M⁻¹ cm⁻¹
ε / M⁻¹ cm⁻¹
Wavelength /nm
5
4
3
2
1
0
-1
-2
-3
-4
-5
70,000
60,000
50,000
40,000
30,000
20,000
10,000
0
150
200
250
300
350
400
450
500
550

(*h*)

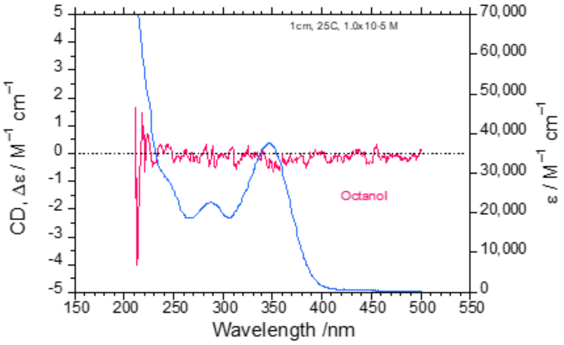
1cm, 25C, 1.0x10-5 M
Octanol
CD, Δε / M⁻¹ cm⁻¹
ε / M⁻¹ cm⁻¹
Wavelength /nm
5
4
3
2
1
0
-1
-2
-3
-4
-5
70,000
60,000
50,000
40,000
30,000
20,000
10,000
0
150
200
250
300
350
400
450
500
550

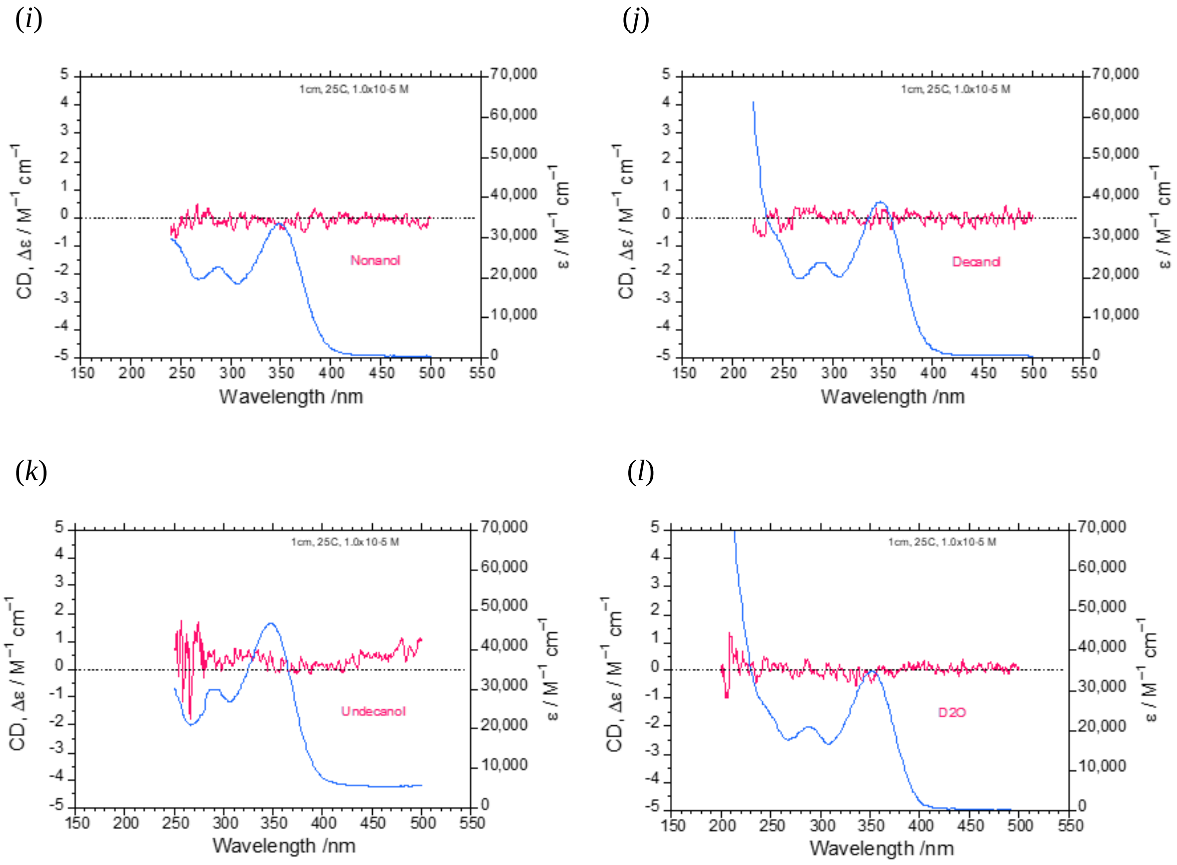

Fig. S11: CD spectra of **PP** in Methanol (a), Ethanol (b), *n*-Propanol (c), *n*-Butanol (d), *n*-Pentanol (e), *n*-Hexanol (f), *n*-Heptanol (g), *n*-Octanol (h), *n*-Nonanol (i), *n*-Decanol (j), *n*-Undecanol (k), D_2O (l).

3. Calculation of Transition Dipole Moment:

According to the purtubation therory[2] (*J. Mol. Struct. Theo. Chem.*, 2004, *678* (1–3), 177–181):

$$\tilde{\upsilon}_a - \tilde{\upsilon}_f = m_1 f(\varepsilon, n) + Const \qquad (1)$$

$$\tilde{\upsilon}_a + \tilde{\upsilon}_f = -m_2 \left[f(\varepsilon, n) + 2g\,(n)\right] + Const. \qquad (2)$$

Where $\tilde{\upsilon}_a$ and $\tilde{\upsilon}_f$ are the frequency of absorption and emission, respectively. The ε is dielectric constant of the solvent, n is the refractive index of the solvent and m_1 and m_2 are slopes of respective straight line equations. The solvent polarity factor f(ε, n) and g(n) are described in equation (3) and (4).

$$f(\varepsilon, n) = \frac{2n^2+1}{n^2+2}\left[\frac{\varepsilon-1}{\varepsilon+2} - \frac{n^2-1}{n^2+2}\right] \qquad (3)$$

$$g(n) = 3/2\left[\frac{n^4-1}{(n^2+2)^2}\right] \qquad (4)$$

The dipole moments at the ground state (μ_g) and excited state (μ_e) can be calculated using the eq. (5) and (6).

$$\mu_g = \frac{m_2 - m_1}{2} \sqrt{\frac{hca^3}{2m_1}} \tag{5}$$

$$\mu_e = \frac{m_2 + m_1}{2} \sqrt{\frac{hca^3}{2m_1}} \tag{6}$$

Where *h* is Planck's constant, *c* is speed of light and *a* is Onsager radius which was calculated using the dimensions taken from DFT optimized structures of luminophores (*J. Phys. Chem.* 1994, *98* (11), 2809–2812).

Table S1: Table of solvent parameters.

Solvent	f(ε,n)	f(ε,n)+2g(n)
Methanol	0.857	1.305
Ethanol	0.821	1.303
Propanol	0.781	1.305
Butanol	0.749	1.291
Pentanol	0.716	1.273
Hexanol	0.686	1.254
Heptanol	0.652	1.227
Octanol	0.614	1.196
Nonanol	0.588	1.177
Decanol	0.553	1.146
Undecanol	0.455	1.051

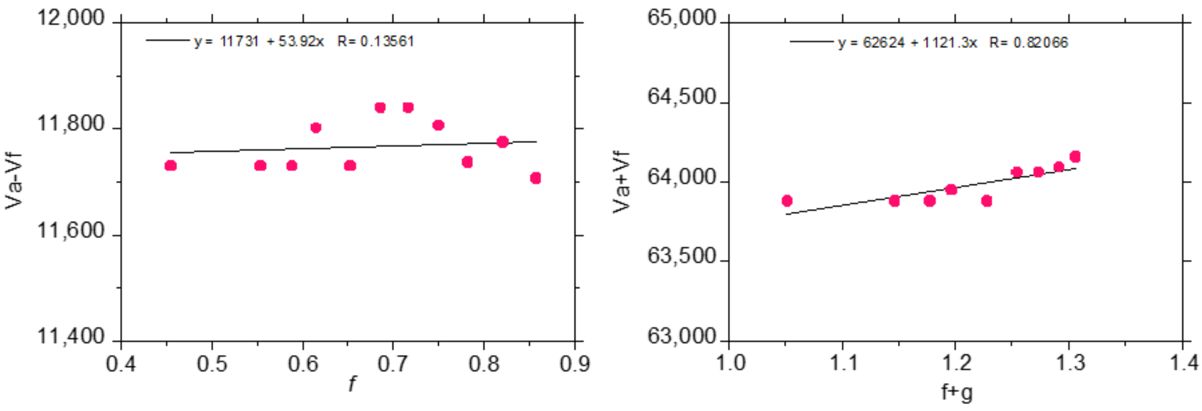

Fig. S12: Plot of v_a-v_f vs. f(ε, n) and v_a+v_f vs. f(ε, n)+2g(n) for **DSA** in various alcohols.

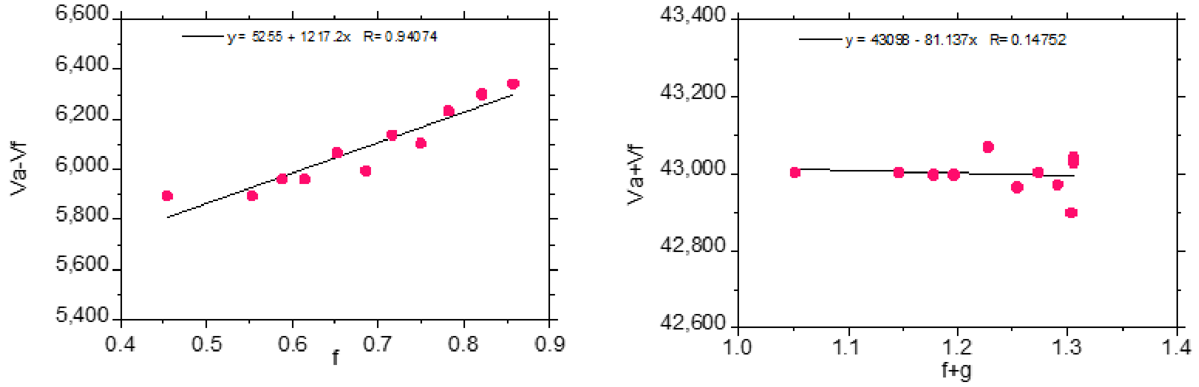

Fig. S13: Plot of v_a-v_f vs. f(ε, n) and v_a+v_f vs. f(ε, n)+2g(n) for **DSBA** in various alcohols.

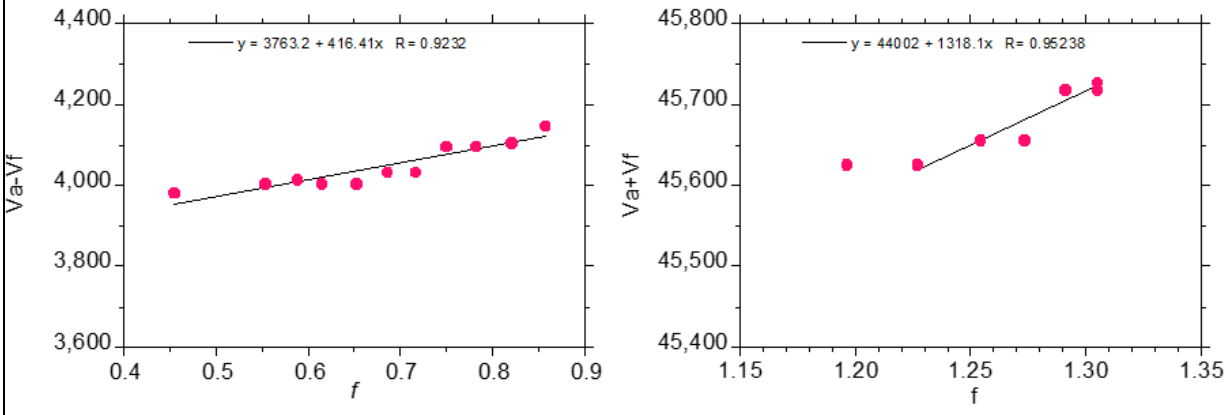

Fig. S14: Plot of v_a-v_f vs. f(ε, n) and v_a+v_f vs. f(ε, n)+2g(n) for **DSBP** in various alcohols.

Table S2: Table of transition dipole moment values for **DSA**, **DSBA**, and **DSBP**.

Sample	m_1	m_2	μ_g	μ_e	$\Delta \mu$
DSBA	41641	-131811	-16.1408	-8.39089	7.74992
DSBP	5392	-112131	-30.432	-27.6395	2.792459
DSA	121719	8113	-4.5083	5.15221	9.660513

4. Time-Resolved Photoluminescence and Quantum Efficiency:

Table S3: Table of K_f, Φ and τ values of **DSA** in selected solvents.

Solvent	K_f	Φ	τ/nsec
Ethanol	0.0051	0.02	3.9041
Pentanol	0.01405	0.04	2.8472
n-Octanol	0.01509	0.04	2.65
n-Undecanol	0.02278	0.06	2.6335

Table S4: Table of K_f, Φ and τ values of **DSBA** in selected solvents.

Solvent	K_f	Φ	τ//nsec
Ethanol	0.03405	0.122	3.5829
n-Pentanol	0.04141	0.143	3.4529
n-Octanol	0.04206	0.141	3.3522
n-Undecanol	0.0528	0.167	3.1631

Table S5: Table of K_f, Φ and τ values of **DSBP** in selected solvents.

Solvent	K_f	Φ	τ//nsec
Ethanol	0.02514	0.029	1.1535
n-Pentanol	0.01938	0.02	1.0317
n-Octanol	0.03017	0.029	0.96112
n-Undecanol	0.0263	0.023	0.872

The photoluminescence quantum efficiency (PLQE) of each sample was evaluated by the formulae, $\Phi_{\text{unk}} = \Phi_{\text{std}}\ [\{A_{\text{std}} / I_{\text{unk}}\}/ \{A_{\text{unk}} / I_{\text{std}}\}]\ \{n_{\text{D,unk}} / n_{\text{Dstd}}\}$, where Φ_{unk} is PLQE of unknown sample, Φ_{std} is PLQE of standard sample (in this case, 9,10-diphenylanthracene was used as standard), A_{std} is absorbance maxima of standard sample, A_{unk} is absorbance maxima of unknown sample, I_{unk} is peak area intensity of emission spectra of unknown sample, I_{std} is peak area intensity of emission spectra of standard sample.

5. Solid state emission of **DSA**, **DSBA**, and **DSBP**:

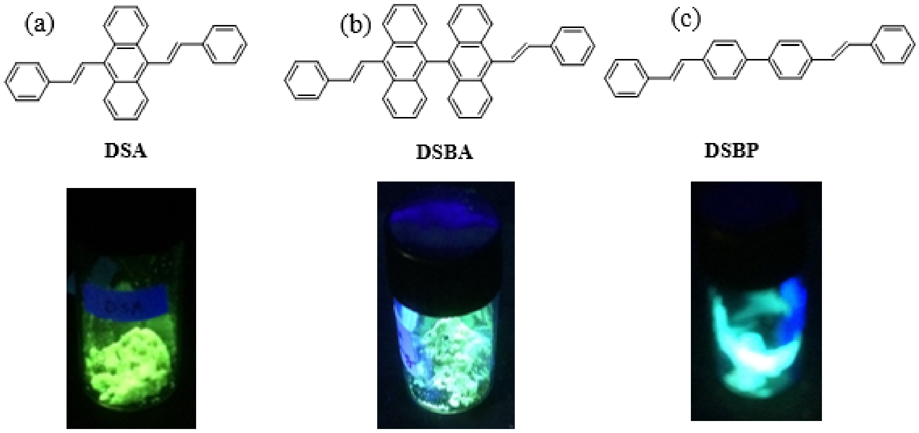
(a)
DSA
(b)
DSBA
(c)
DSBP
DSA

Fig. S15: Photographs of solid state emission of DSA (a), DSBA (b) and DSBP (c).

6. DFT Calculations:

Table S6: Optimized structure, HOMO and LUMO of **DSA**, **DSBA**, and **DSBP** with DFT calculations using Gaussian 09 (6-311G, B3LYP).

	DSA	DSBA	DSBP
Optimized structure	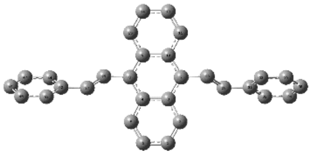	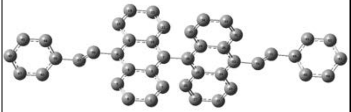	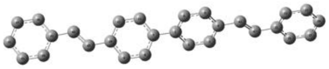
HOMO	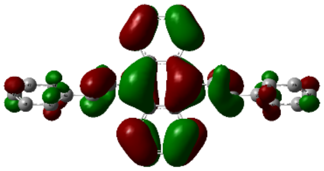	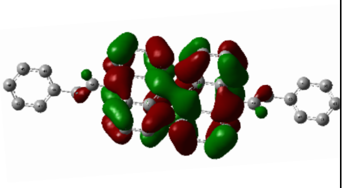	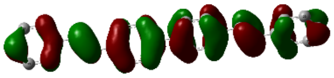
LUMO	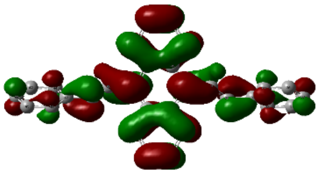	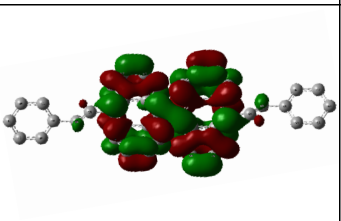	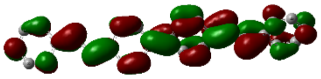

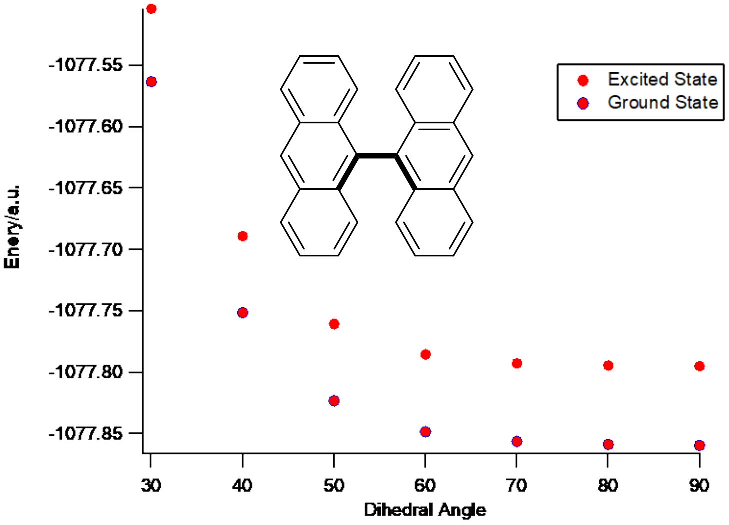

Fig. S16: Graph of forced dihedral angle vs. ground state energy of **BA**.

7. CPL of **DA** and **PP** vs. Viscosity:

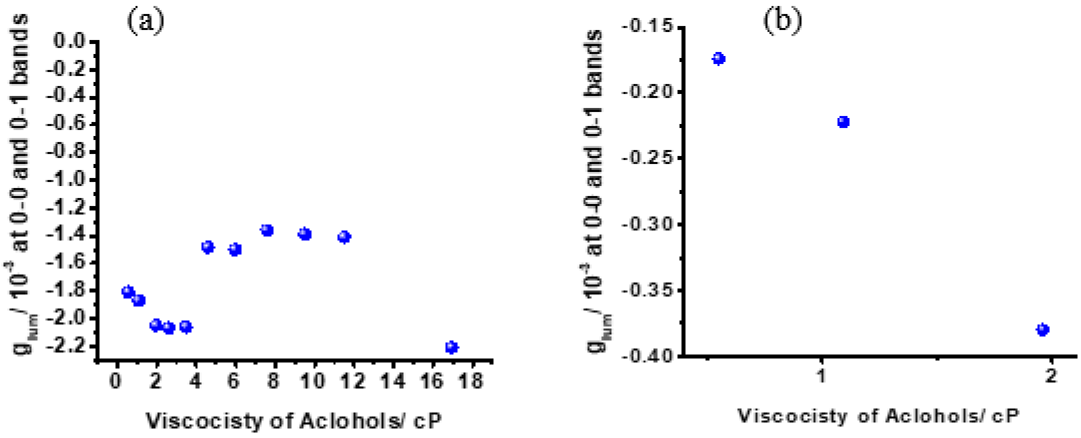

Fig. S17: Graph of g_{lum} vs. viscosity of the solvent for **DA** (a) and **PP** (b).

8. Analysis of *cis*-*trans* isomerization of **DSA** luminophores:

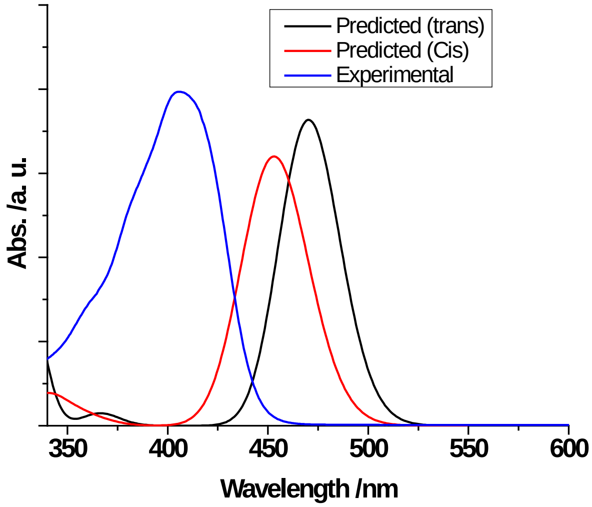

Fig. S18: Experimental and predicted UV-Vis spectra of **DSA** with TD-DFT (B3LYP, 6-311G basis set).